ADDIS ABABA UNIVERSITY

SCHOOL OF GRADUATE STUDIES

DEPARTMENT OF CHEMISTRY

GRADUATE PROJECT (Chem.774)

Fluorene-Based Alternating Copolymers: Synthesis and Characterization

Advisor: Wendimagegn Mammo (Professor)

By

Zewdneh Genene

A Graduate Project Submitted in Partial Fulfillment of the Requirements for the Degree of Master of Science in Chemistry

July 2010

Declaration

I, the undersigned, declare that this MSc project is my original work and has not been presented for any degree in any other university and that all sources of materials used for this project have been duly acknowledged.

Name: **Zewdneh Genene**

Signature: _____

This MSc. project has been submitted for examination with my approval as a university advisor.

Name: **Wendimagegn Mammo (Professor)**

Signature: _____

Date and place of submission: Department of Chemistry

Addis Ababa University

July 2010

ADDIS ABABA UNIVERSITY

SCHOOL OF GRADUATE STUDIES

DEPARTMENT OF CHEMISTRY

GRADUATE PROJECT (Chem.774)

Fluorene-Based Alternating Copolymers: Synthesis and Characterization

Submitted by **Signature**

Zewdneh Genene _____

Approved by the Examining Board: **Signature**

Prof. Wendimagegn Mammo _____

Advisor

Prof. Ermias Dagne _____

Examiner

Dr. Gizachew Alemayehu _____

Examiner

Acknowledgements

I would like to express my deepest gratitude to my project supervisor, Professor Wendimagegn Mammo, for all his unreserved guidance, technical and moral support, and encouragement during the entire project work and preparation of the paper.

I would like to extend my deepest gratitude to Desta Anteneh for running NMR spectra of almost all compounds, encouragements and for always making my work in the laboratory fruitful.

My gratitude gose to Dr. Shimelis Admassie for characterizing the synthesized polymers by running CV and UV-vis spectroscopy.

I would also like to thank Yoseph Atilaw for running the NMR spectra of some compounds.

I am grateful to my colleagues, Mekonnen Abebayehu, Endale Mulegeta for their assistance on countless occasions, and to my friends and family for their ongoing support.

Ambo University is gratefully acknowledged for giving me full scholarship for my M.Sc. study.

Addis Ababa University, department of Chemistry is also acknowledged for providing the laboratory space and the necessary chemicals to conduct the research work.

Table of contents

List of Schemes

List of Tables

List of Figures

List of Abbreviations

DMF: N,N-Dimethyl formamide

ACOH: Acetic acid

NMR: Nuclear Magnetic Resonance

HOMO: Highest Occupied Molecular Orbital

LUMO: Lowest Unoccupied Molecular Orbital

^{o}C: Degree Celsius

h: Hour(s)

min: Minutes

%: Percentage

J: Coupling constants

d: Doublet

m: Multiplet

dd: Doublet of doublets

t: triplet

ppm: Parts per million

NBS: *N*-Bromosuccinamide

TBAF: Tetrabutylammonium fluoride

THF: Tetrahydrofuran

TEAOH: Tetraethyl ammonium hydroxide

PF: Polyfluorene

APFO: Alternating polyfluorene

PLED: Polymer light emitting diodes

PL: Photoluminescence

EL: Electroluminescence

LEC: light emitting electrochemical cells

Abstract

Alternating polyfulorene copolymers, which have donor-acceptor-donor segments in between the fluorene segments were synthesized and characterized. The donor-acceptor-donor monomers, namely, 5,8-bis(5-bromothiophen-2-yl)-2,3-bis(3-(tert-butyl dimethylsilyloxy)phenyl)quinoxaline and 5,8-bis(5-bromothiophen-2-yl)-2,3-bis(3-(2-(2-methoxyethoxy) ethoxy)phenyl)quinoxaline were prepared starting from 3-bromophenol and 2,1,3-benzothiadiazole. The polymers were synthesized by using Suzuki coupling polymerization reaction. The resulting polymers showed good solubility in chloroform. The electrochemical behaviors of the copolymers were characterized by cyclic voltammetry. The synthesized compounds were characterized using spectroscopic techniques.

1. INTRODUCTION

Environmental issues such as fossil fuel shortage and global warming have gained worldwide acknowledgment, and the need for clean renewable energy becomes more urgent as we enter the 21th century. Among all renewable energy sources, solar energy, which is clean, abundant, and virtually limitless, has been extensively studied in recent years. Polymer-based photovoltaics being one of the third-generation solar cell technology, offers advantages of lightweight, high-throughput manufacture, and environmentally benign for portable energy applications.

The term polymer is derived from the Greek's '*poly*' and '*mers*' meaning many parts. Some prefer the term macromolecule or large molecule. Polymers serve as the basis of life in the form of nucleic acids, proteins and polysaccharides. They permit replication, energy transformation, transmission of foods within plants and animals, act as essential natural building materials. Polymers have served as the very building blocks of society-clays for jars, wood for fuel, hides for clothing, vegetation for food and shelter. They are present in a variety of forms-as fibers and cloths, paper, lumber, elastomers, plastics, coatings, adhesives, ceramics, enzymes, DNA, concretes, and are major ingredients in soils and plant life. The basic concepts of polymer science apply equally to natural and synthetic polymers and to inorganic and organic polymers, and as such are important in medicine, nutrition, engineering, biology, physics, mathematics, computers, environment, space, ecology, and health[1].

Currently, conjugated polymers have received a great deal of attention from both academia and industry because of the numerous applications for which they are potentially useful. Photovoltaic devices [2], light-emitting diodes (LEDs) [6], field effect transistors [3], electrochromic devices [4], and numerous types of sensors [5] based on conjugated polymers are actively being pursued as viable technologies. Figure 1 shows some examples of conjugated polymers. The great interest in this class of materials is rooted in the combination of semiconducting characteristics, polymeric material properties, and the organic structural basis that defines conjugated polymers. Although

the optical, electronic, and material properties are the focus for applications, the underlying synthetic organic flexibility is the most attractive feature of conjugated polymers. Through the manipulation of the monomeric and polymeric structures, the physical, optical, and electrochemical properties can be tuned for specific applications.

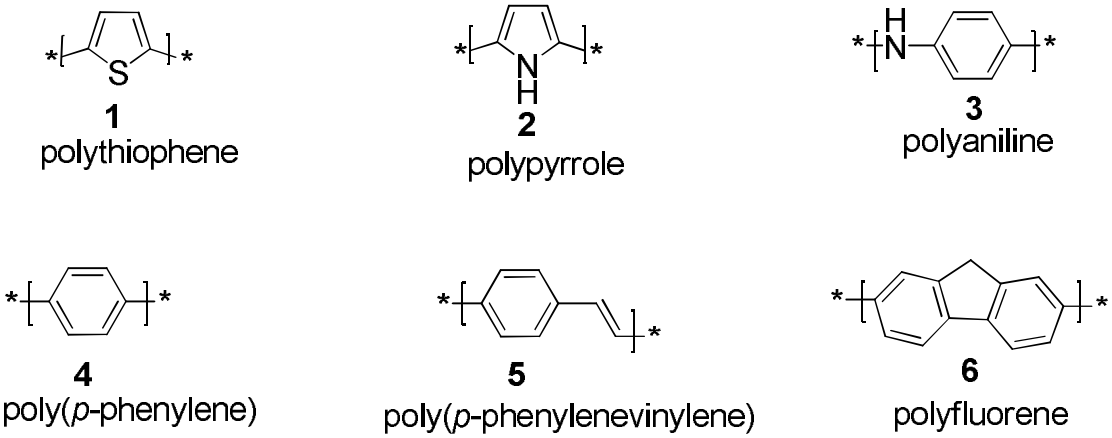

Figure 1. Chemical structures of some conjugated polymers

Band-gap is an important tunable property of conjugated polymers. For many applications, such as LEDs and photovoltaics, the value of the band-gap is pivotal because it determines the color of the emitted light in LEDs and the effectiveness with which solar radiation is absorbed in photovoltaic devices. The structural basis for manipulating the magnitude of the band-gap has been thoroughly investigated and reviewed [6].

One important synthetic target has been the development of low-band-gap conjugated polymers. Low-band-gap polymers are promising candidates for solar cells [7] as well as *n*-type conductors and multicolor electrochromic polymers [8]. Among the successful approaches to a low-band-gap system, the donor–acceptor approach has received significant attention. In this approach, the combination of an electron-rich donor and an electron-deficient acceptor results in a conjugated polymer with a compressed band-gap. Due to an intra-chain charge transfer from donor to acceptor, the high energy level for the highest occupied molecular orbital (HOMO) of the donor and the low energy level

for the lowest unoccupied molecular orbital (LUMO) of the acceptor results in a lower band-gap. By carefully selecting the appropriate structures of the donor and acceptor, it is possible to tune the magnitude of the band-gap, the absolute energies of the frontier orbitals, and the solubility of the resulting polymer [9].

Low band-gap polymer-based donor-acceptor strategy has centered on the use of nitrogen-containing heterocycles as effective acceptors. Heterocycles such as pyridine and quinoxaline, which contain an imine nitrogen are electron-deficient and thus serve as efficient electron acceptors [10]. In specific examples, band-gaps as low as 0.3 and 0.5 have been reported for electropolymerized donor–acceptor–donor polymers with thiophene as the donor and either thiadiazolothienopyrazine or benzothiadiazole as the acceptor [11,12]. The other advantage of incorporating electron-deficient *N*-heterocycles into a conjugated polymer is that the lowest unoccupied molecular orbital (LUMO) energy of a conjugated polymer will be lowered because of the presence of the more electronegative nitrogen atom [13]. As such, the resulting polymer will be easier to reduce, more likely to exhibit reversible *n*-type doping, and show higher levels of electron mobility. Such a polymer could serve as an efficient electron-accepting material in photovoltaic devices or as an electron-transport material in LEDs.

2. LITERATURE REVIEW

Donor–acceptor conjugated polymer systems have emerged as promising candidates for organic solar cells and photodiodes. The development of N-heterocycle based donor–acceptor polymers offers an attractive target. Several groups have developed such systems based on the copolymerization of donor and acceptor monomers to yield alternating donor–acceptor copolymers. These systems are primarily based on thiophene as a donor and pyridine, quinoxaline, or pyridopyrazine as an acceptor.
Incorporating such acceptor units into polythiophenes and polyfluorenes are expected to shift the HOMO energy level towards lower energies resulting in a higher stability of the polymers against oxidation and photooxidation, and to lower the HOMO–LUMO energy gap which allows the absorption of an enlarged portion of the sunlight [14]. Herein, alternating copolymers based on quinoxaline and fluorene have been reviewed.

2.1. Quinoxaline monomeric sub-units

A quinoxaline, also called a benzopyrazine, is a heterocyclic compound containing a ring made up of a benzene ring and a pyrazine ring. Among the various classes of nitrogen containing heterocyclic compounds, quinoxaline derivatives are important components of several pharmacologically active compounds [15].

Quinoxaline-containing building blocks are also extensively used in the chemistry of photoluminescent molecules, electroluminescent materials and organic semiconductors because they usually display high electron affinities, good thermal stabilities [16], and they may also act as electron-transporting materials. These derivatives have been successfully incorporated into polymers for use as electron-transport materials in multilayer organic LEDs [17].

A number of synthetic strategies have been developed for the preparation of substituted quinoxalines [18,19]. The most common method relies on the condensation of an aryl 1,2-diamine with a 1,2-dicarbonyl compound in refluxing ethanol or acetic acid for 2 - 12

hours giving 34–85% yields [20]. The quinoxaline monomer (**10**) was prepared in a multistep procedure as depicted in Scheme 1 following this strategy. 1,4-Dibromo-2,3-diaminobenzene (**9**) was prepared starting from benzo[*c*][1,2,5]thiadiazole (**7**) and subsequently condensed with symmetric 1,2-diketones to yield the corresponding dibromoquinoxalines (**10**) [14].

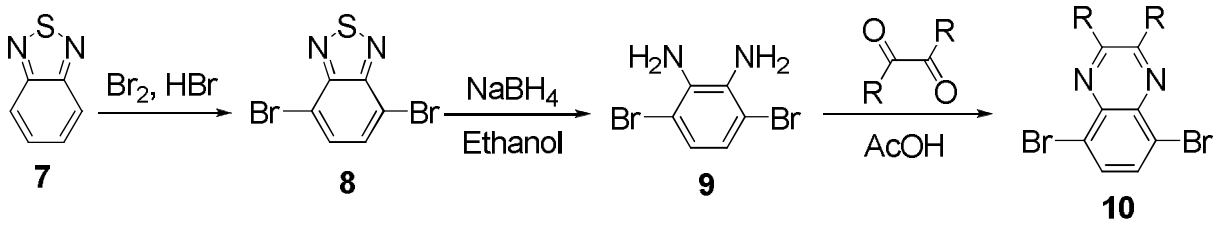

Scheme 1. Syntheis of dibromoquinoxalines (**10**)

Dibromoquinoxalines (**10**) have been used as precursors for the synthesis of thiophene–based alternating donor-acceptor copolymers. Polymers **12** were prepared by Stille copolymerization of 2,5-bis(trimethylstannyl)thiophene (**11**) with dibromoquinoxalines (**10**) using a Pd(0) catalyst [21]. The Stille coupling reactions between trimethyl(thiophen-2-yl)stannane and dibromoquinoxalines (**10**) in the presence of catalytic amount of Pd(II) afforded monomers **13**, which were electropolymerized to polymers **14** (Scheme 2).

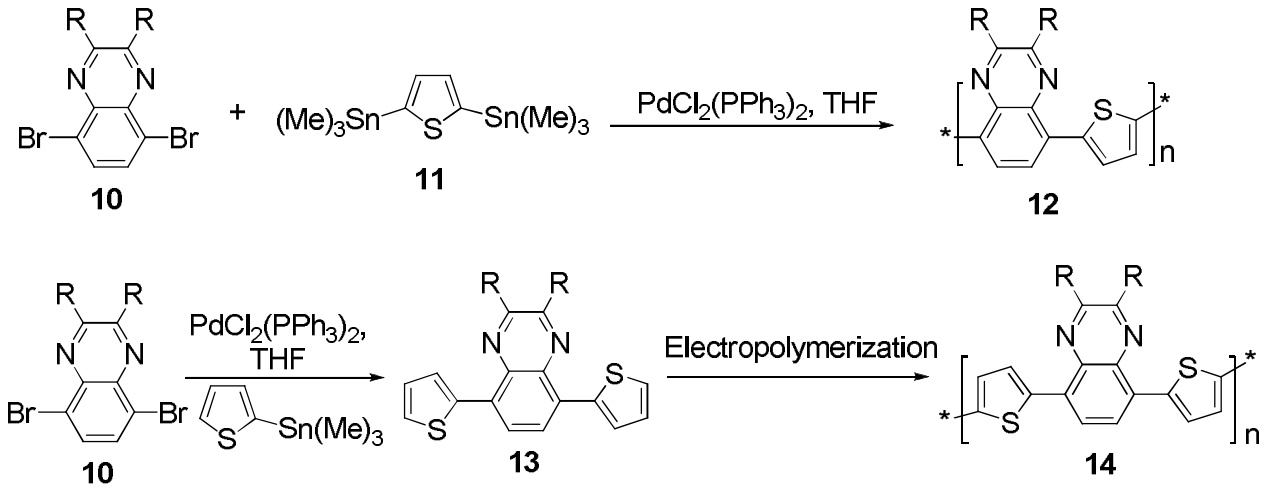

Scheme 2. Synthesis of alternating quinoxaline/thiophene copolymers

Recently, a new class of π-conjugated heterocyclic polymers of poly(quinoxaline) derivatives were explored as electron transporting or electron accepting materials because of their high electron affinity due to the two symmetric unsaturated nitrogen atoms in quinoxaline. To develop new materials based on quinoxaline, two-dimensional donor-acceptor conjugated copolymers consisting of electron-deficient quinoxaline subunit as electron-acceptor core and *p*-phenylenevinylene or thiophene as electron-donor groups in the main chain, were designed and synthesized [22] (Scheme 3). To avoid polymerization of styrene, monomer **18** was quickly reacted with monomer **17** by Heck coupling reaction to afford polymer **19**; while polymer **21** was obtained from monomer **17** and **20** by Stille coupling reaction.

In polymers **19** and **21,** because electron-deficient quinoxaline is connected by electron-donor groups, both in side chains and main chains through conjugated linkage, electrons could transfer easily from electron-donor groups to quinoxaline core and delocalize all over the phenyl rings lying in the chains. The unusual topological structure makes the polymers possess low band-gap and broad absorption, which could be beneficial to harvest light efficiently for photovoltaic conversion [22].

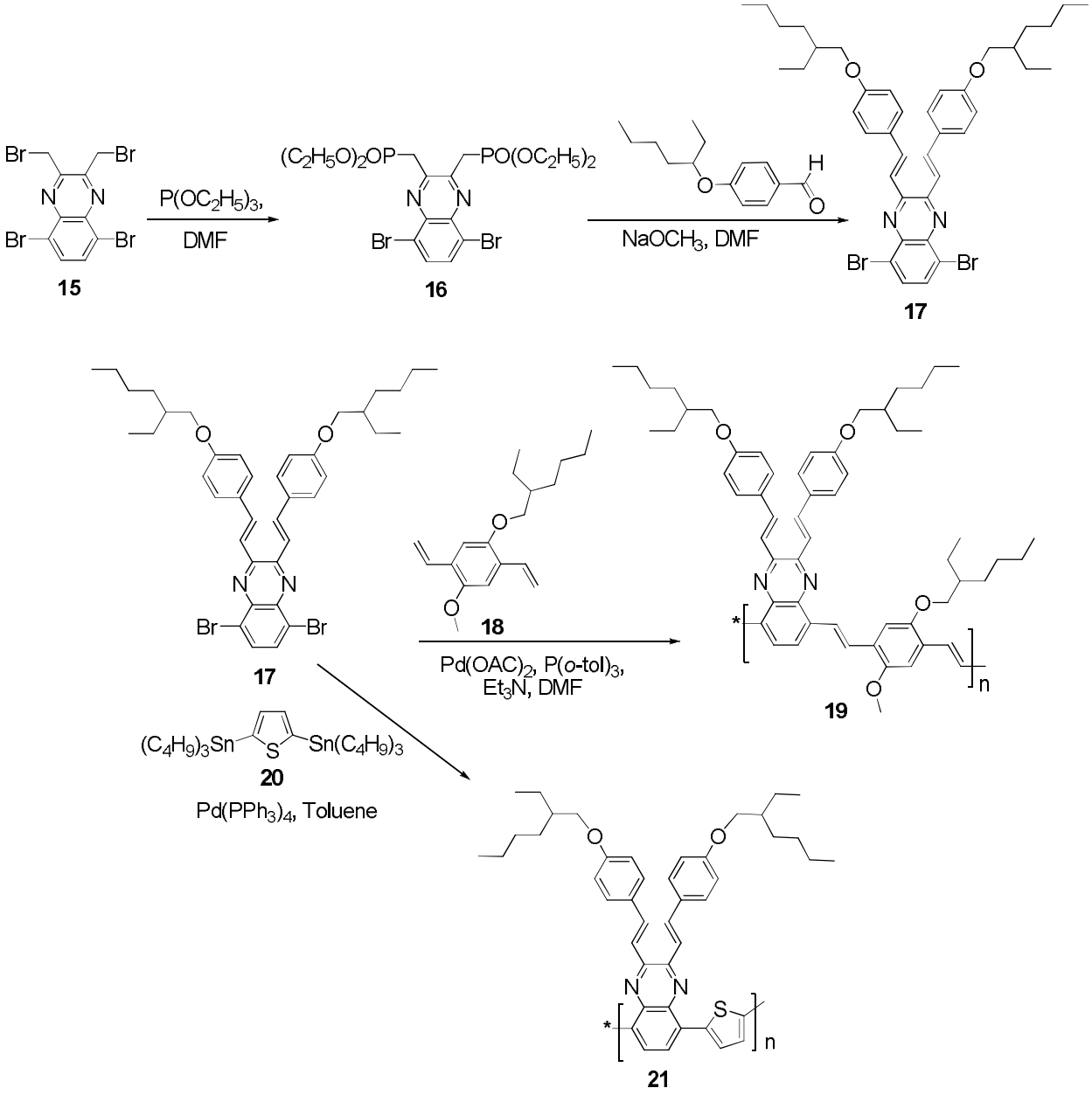

Scheme 3. Synthesis of polymers **19** and **21**

2.2. Fluorene-based monomers

Polyfluorenes are well known blue-emitting materials and have high luminescence efficiency, excellent thermal and oxidative stability and good processability [23].

Fluorene or 9*H*-fluorene (**22**) is an isocyclic aromatic hydrocarbon composed of two benzene rings that are connected via a direct carbon–carbon bond and an adjacent methylene bridge. The methylene bridge forces the two phenyl rings to be planar [24], which increases their orbital overlap and the degree of conjugation of the aromatic system. It has a violet fluorescence, hence its name. In bare fluorene, the protons at the sp^3 carbon in the methylene bridge (9-position) exhibit a significant CH acidity (p^{KA} = 22.98) as the resulting aromatic fluorenyl anion is efficiently resonance-stabilized [25]. Due to this acidic protons, fluorenes can undergo oxidation and alkylation reactions at the 9-position.

There are different synthetic approaches to 9,9-dialkyl-substituted fluorene monomers. The most commonly used reactions are nucleophilic substitutions using alkyllithium reagents (Scheme 4), and phase transfer catalysis reactions (Scheme 5). The former uses a strong base like *n*-butyllithium (*n*-BuLi) in dry THF at -78 ^{o}C to deprotonate the acidic proton from the benzyilic positions to form 9-fluoryllithium, which is resonance stabilized anion and consequently, the resulting alkyl lithium acts as a nucleophile to undergo nucleophilic substitution reaction with an alkyl halide [26].

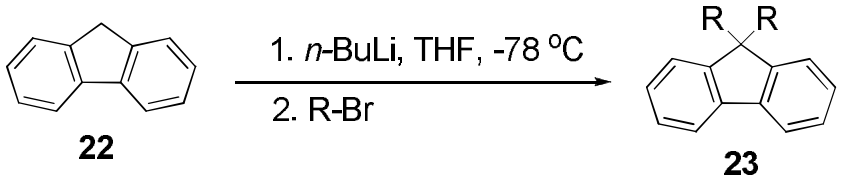

Scheme 4. Alkylation of fluorene by nucleophilic substitution reaction

The phase transfer catalysis reaction involves the use of a two-phase system composed of equal volumes toluene and aqueous NaOH solution [27] and tetraalkylammonium bromide as phase transfer catalyst (Scheme 5).The advantage of this reaction over the nucleophilic substitution reaction is that it can be implemented on a 2,7-dihalogenated fluorene and it avoids the risk of halogenating the side chain and unwanted reactions on functional groups of the side chain.

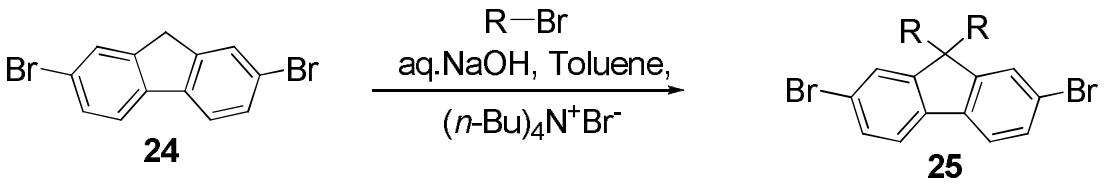

Scheme 5. Alkylation of fluorene by phase transfer catalysis reaction

9,9-Dialkyl-2,7-dibromofluorene (**25**) can be used as a monomer for the synthesis of polymers and as precursor for the synthesis of the corresponding diboronic acids or boronate esters, which can be polymerized through the Suzuki-type polymerization route with dihaloaryls. The synthesis of 9,9-dialkyl-9*H*-fluorene-2,7-diyldiboronic acids or the corresponding boronate esters uses a very strong base like *n*-BuLi for the formation of the aryllithium reagents through halogen-metal exchange. Subsequent treatment of the resulting aryllithiums with tributylborate affords the 9,9-dialkyl-9*H*-fluorene-2,7-diyldiboronic acids (**26**) after an acid work-up whereas treatment with pinacolborane affords ,9-dialkyl-9*H*-fluorene -2,7-diboronate esters (**27**) as shown in Scheme 6.

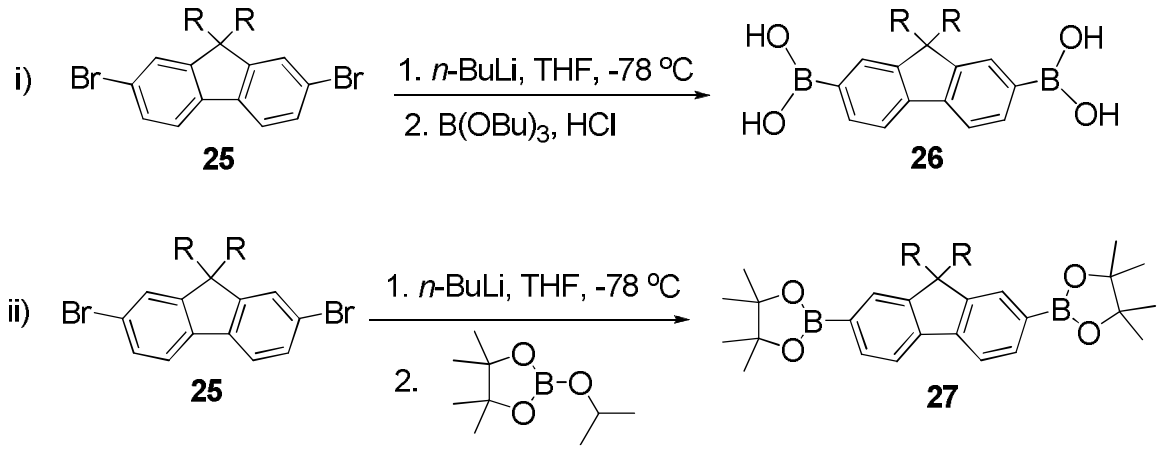

Scheme 6. Synthesis of (i) fluorene-2,7-diboronic acids (**26**) and (ii) fluorene-2,7-diboronate esters (**27**)

2.3. Fluorene-based polymers

The synthesis of polyfluorenes (PFs) and their derivatives have been thoroughly studied. The first synthesis of soluble PFs was reported in 1989 by the oxidative coupling of dihexylfluorene with $FeCl_3$. The material obtained, however, had a low-molecular weight and additionally contained structural defects, as the oxidative coupling does not proceed strictly regioselectively [28]. An enormous synthetic improvement was the introduction of metal-catalyzed aryl–aryl coupling reactions that require monomers functionalized in the 2 and 7 positions, since they guarantee perfect regioselectivity. The most prominent types of reactions used to prepare PFs are the Ni(0)-mediated Yamamoto and the Pd-catalyzed Suzuki condensations [24, 29] (Scheme 7). If the appropriate reaction conditions are applied, high molecular weight PFs can be obtained with both strategies.

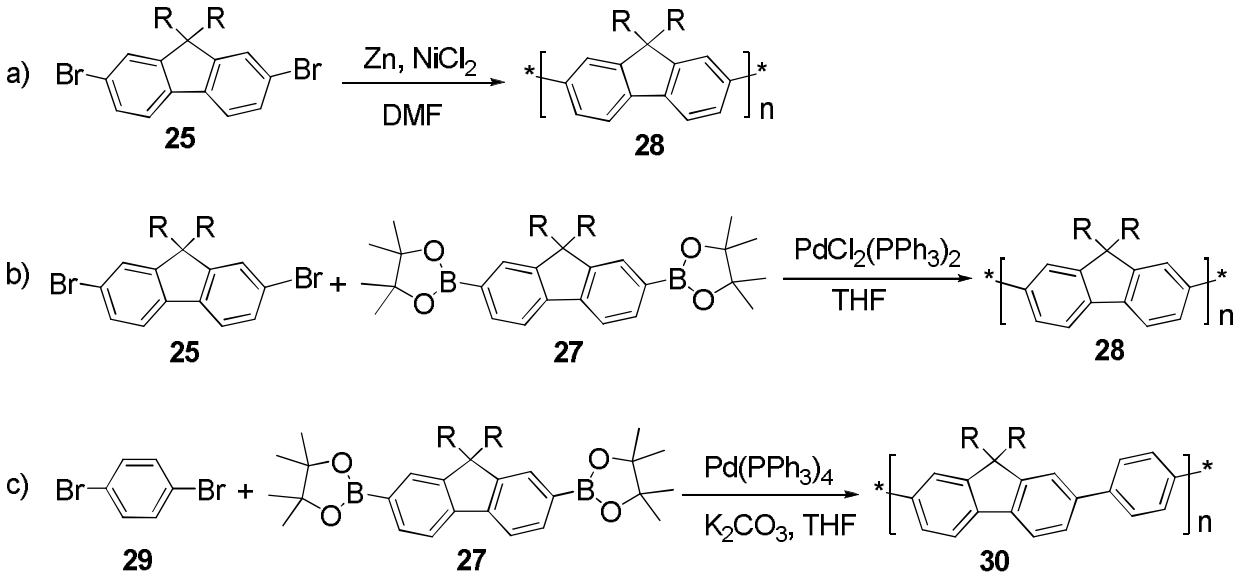

Scheme 7. Synthesis of polyfluorenes (a) Yamamoto reaction (b) Suzuki coupling reaction (c) alternating polyfluorene synthesis by Suzuki coupling reaction

Although copolymers can be prepared via the Yamamoto route, the Suzuki coupling reaction is the standard procedure used, because it allows the synthesis of strictly

alternating polyfluorene copolymers (APF) (Scheme 7), which have especially advantageous material properties [30].

The homopolymers of substituted polyfluorene have large band-gaps (*ca* 3.68 eV) and have been used as a blue light emitters in light emitting diodes [30, 31]. However, the light emitted and hence the band-gap of polyfluorene could be tuned with addition of different electron donating or electron accepting units in the back bone of the polymer [32].

The past few years have seen a tremendous increase in the preparation of polyfluorene copolymers incorporating alternating donor-acceptor units. **APFO-3** is a copolymer based on thiophene, benzothiadiazole and fluorene and is an example of the alternation of the electron donating thiophene/fluorene unit, and the electron accepting benzothiadiazole unit, (Figure. 2). The band-gap **of APFO-3** was estimated from its UV-Vis spectrum to be 2.01 eV. Hou *et al*. found that due to exciton trapping in the benzothiadiazole unit, efficient charge transfer was achieved [31].

Copolymers based on thiophene, fluorene and thienopyrazine, quinoxaline or thiadiazoloquinoxaline are other examples of the alternation of the electron donating unit, thiophene/fluorene, and the electron accepting unit, thienopyrazine, quinoxaline or thiadiazoloquinoxaline. **APFO-Green1**, **2**, **3**, **4** and **5** (Figure 2) are representative examples containing the above structural units [32, 33]. The reported band-gap for instance, for **APFO-Green2** was 2 eV, and its λ_{max} was located at 380 and 615 nm [34].

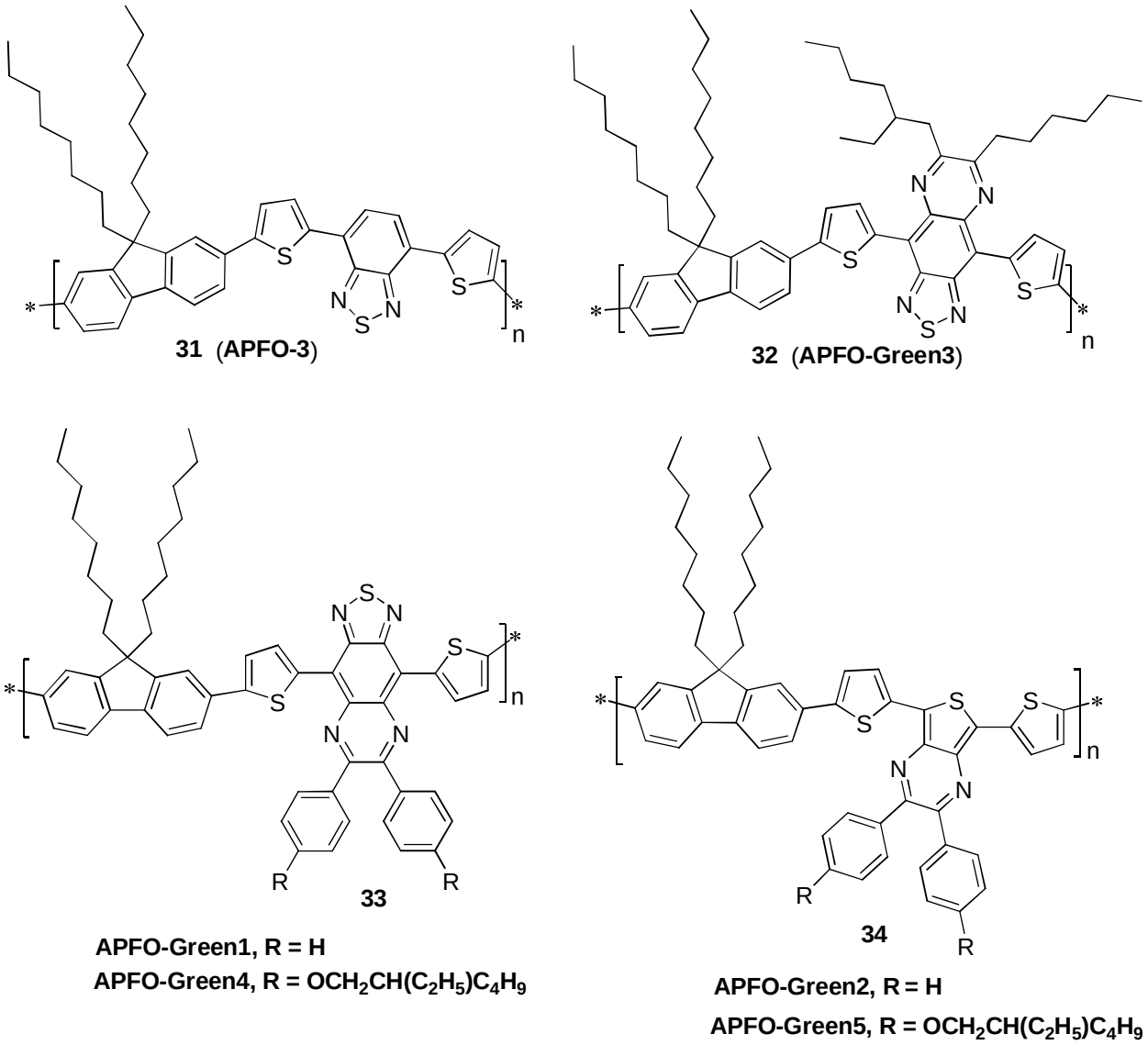

Figure 2. Structures of **APFO-3**, **APFO-Green1**, **2**, **3**, **4** and **5**.

Other examples of copolymers based on fluorene and different quinoxaline units have been published. Poly[2,7-(9,9-dioctylfluoren)-*alt*-5,5-(5',8'-di-2-thienyl-(2',3'-bis-(3'-octyloxyphenyl)-quinoxaline))] (**35**) (**APFO-15**), belongs to this class of compounds. (Figure 3). The absorption of the polymer has onset at about 640 nm, while it has two clear peaks located at 542 and 396 nm [35]. The electrochemically determined band-gap of **APFO-15** was 2.7 eV.

Desta G. [36] successfully synthesized **APFO-25** (**36**) by introducing quinoxaline moieties containing alkoxyphenyl and phenol side chains onto the quinoxaline units of PF copolymers (Figure 3). The reported optical absorption of **APFO-25** started at 630 nm with a first local maximum at 534 nm and a second maximum at 390 nm. The optical band-gap was similar to that of **APFO-15**. The electrochemically determined band-gap of **APFO-25** was 2.5 eV.

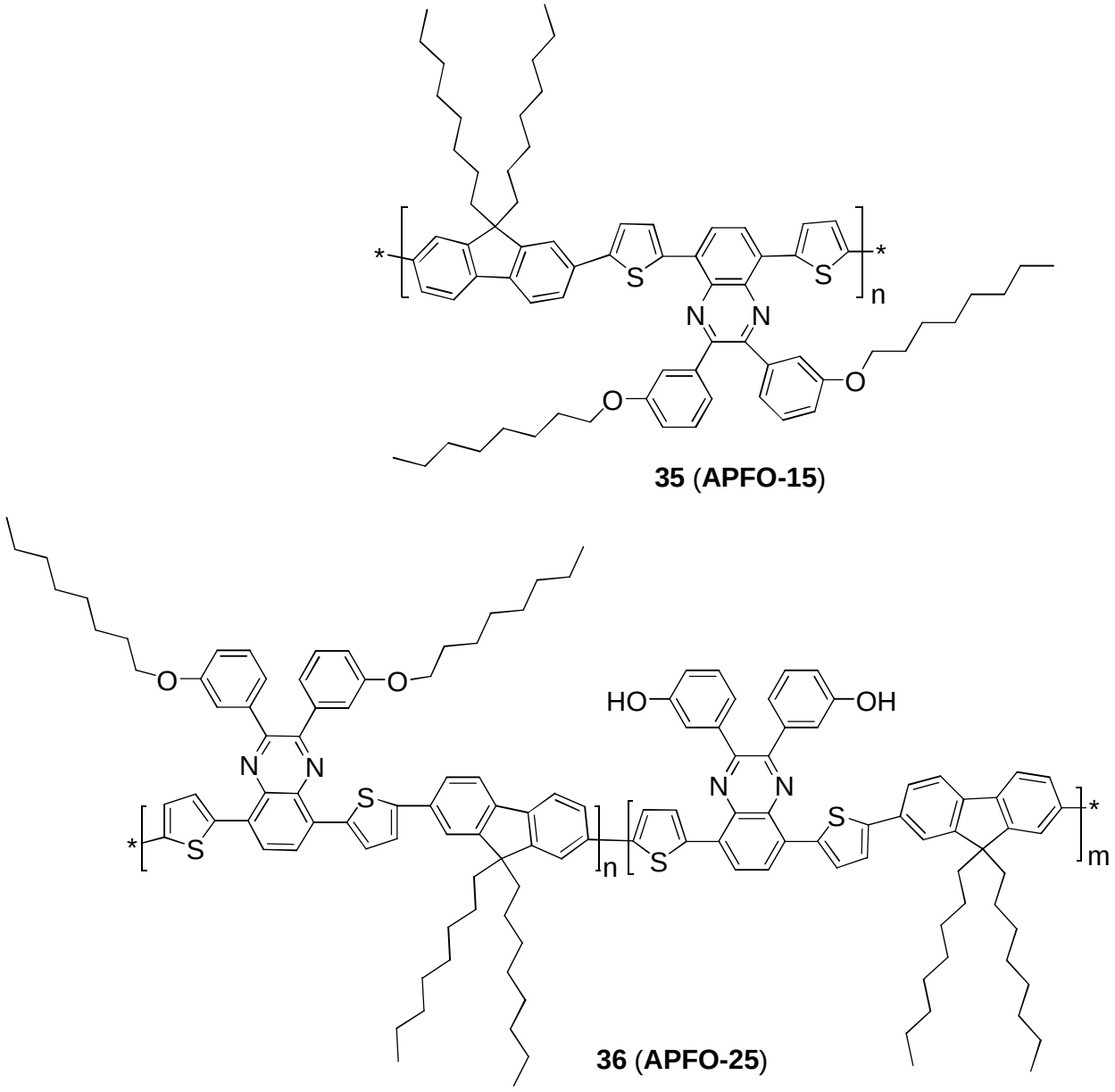

35 (**APFO-15**)

36 (**APFO-25**)

Figure 3. Structures of **APFO-15** and **APFO-25**.

2.4. Optoelectronic Applications

Polyfluorenes combine a number of advantageous properties making them attractive materials for use in polymer electronic devices. High-molecular weight samples are easily accessible via metal-mediated polymerization reactions. Their good solubility in organic solvents allows the use of simple processing techniques such as spin coating and ink jet printing. Furthermore, thin films are flexible and resistant to decomposition upto temperatures above 400 ^{o}C [37].

Because of the rather large band-gap of PF, the main field of application is in blue polymer light-emitting diodes (PLEDs). The color of the electroluminescent light depends on the energy difference between the excited and the ground state and thus blue emission occurs when PF is used as the active layer. The first example of a blue PLED based on PF was published in 1991. It contained poly(dihexylfluorene) and had a rather poor performance [38]. Since then, however, impressive improvements have been achieved and PF-based optoelectronic devices are now believed to have the potential of intermediate-term commercialization.

The alternating polyfluorene copolymers share with PF homopolymers many of their advantageous properties, such as good solubility and thus convenient processability, mechanical flexibility, and thermal stability. Because of their more complex chemical structures, some are synthetically less easily accessible, especially if the comonomers require elaborate multistep preparation. A crucial advantage of APFs compared to PFs is the almost unrestricted tunability of their band-gap energies by the appropriate choice of the comonomer making them attractive for a manifold of applications.

The use of APFs has allowed to extend the range of electroluminescence colors far beyond blue, eventually encompassing the entire visible spectrum. APFs with triaryl amines as copolymers, such as poly(fluorene-*alt*-bis-(alkylphenyl)-bisphenyl-phenylenediamine) (PFB, **37**), combine deep blue emission with good hole mobilities [30]. Increasing the electron acceptor character of the comonomers resulted in green

[39], yellow [40], orange [40], or red [41] PLEDs. White electroluminescence has been achieved by partial energy transfer in blends of blue emitting matrices and lower band-gap APFs [41].

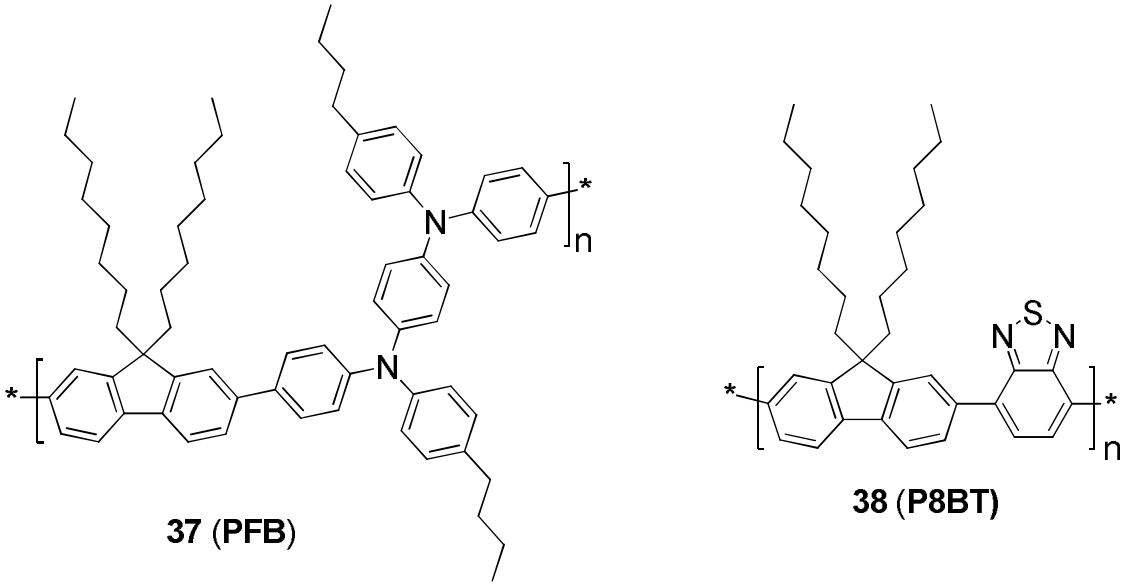

37 (**PFB**) **38** (**P8BT**)

Figure 4. Structures of PFB and P8BT.

The second main field of application of APF is organic photovoltaics [43], either in combination with other polymers or with [6,6]-phenyl-C_{61}-butyric acid methyl ester ([60]PCBM, Figure 5). Because of the broad shape of the solar emission that reaches far into the IR region of the electromagnetic spectrum, efficient solar cells have to collect radiation over a wide range of wavelengths. Poly(fluorene-*alt*-benzothiadiazole) (P8BT, **38**) blended with PFB (**37**) has been used in organic solar cells [44], but due to the rather large band-gaps of P8BT (**38**) (2.3 eV) and PFB (**37**) these devices only collected light of wavelengths shorter than 550 nm. APFs, which are prepared, using mainly thiophene as the donor moiety and various acceptors, like benzothiadiazole, quinoxaline, thienopyrazine, and thiadiazoloquinoxaline are also promising candidates for efficient organic solar cells since they have strong ability to absorb far into the red and even near infrared part of the visible spectrum.

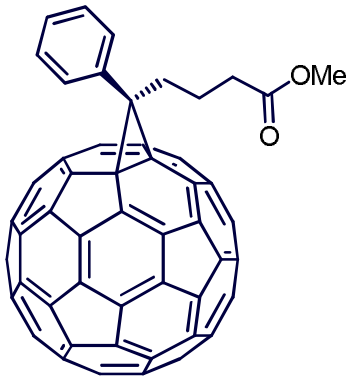

PCBM

Figure 5. The structure of PCBM.

3. OBJECTIVE OF THE PROJECT WORK

The aim of this MSc. project work is to synthesize alternating copolymers of fluorene and donor-acceptor-donor segments. It involves the synthesis of donor-acceptor-donor monomers, namely, 5,8-bis(5-bromothiophen-2-yl)-2,3-bis(3-(tertbutyldimethylsilyloxy) phenyl)quinoxaline and 5,8-bis(5-bromothiophen-2-yl)-2,3-bis(3-(2-(2-methoxyethoxy) ethoxy)phenyl)quinoxaline starting from 3-bromophenol and 2,1,3-benzothiadiazole. These monomers will be polymerized with fluorene-based monomeric units by Suzuki-type polymerization reaction using Pd(0) as catalyst. The intermediate compounds during the synthesis of the monomeric units will be characterized by NMR spectroscopy and the polymers will be characterized by UV-Vis spectroscopy and cyclic voltammetry.

4. RESULTS AND DISCUSSION

4.1. Synthesis of Donor-Acceptor-Donor Segments

The donor-acceptor-donor monomers **48** and **50** were prepared in a multistep procedure. The precursors to build these monomers were the diamine **46** and dione **41** which were synthesized starting from benzo[c][1,2,5]thiadiazole and 3-bromophenol, respectively, as outlined below.

4.1.1. Synthesis of 1,2-bis(3-(*tert*-butyldimethylsilyloxy)phenyl)-ethane-1,2-dione (**41**)

The synthetic route to 1,2-bis(3-(*tert*-butyldimethylsilyloxy)phenyl)ethane-1,2-dione (**41**) is outlined in Scheme 8. Protection of the hydroxyl group of 3-bromophenol (**39**) was carried out in dichloromethane by addition of triethylamine and *t*-butyldimethylsilyl chloride with stirring overnight at room temperature. This resulted in the formation of (3-bromophenoxy)(*tert*-butyl)dimethylsilane (**40**) in 62% yield. Compound **40** was subjected to Grignard reaction with Mg in THF and the resulting Grignard reagent was added to a suspension of LiBr/CuBr mixture. Up on adding oxalyl chloride to the above mixture, 1,2-bis(3-(*tert*-butyldimethylsilyloxy)phenyl)ethane-1,2-dione (**41**) was obtained, which was purified by silica gel column chromatography . Compounds **40** and **41** were characterized based on their ^{1}H-NMR, ^{13}C-NMR, and DEPT-135 spectra.

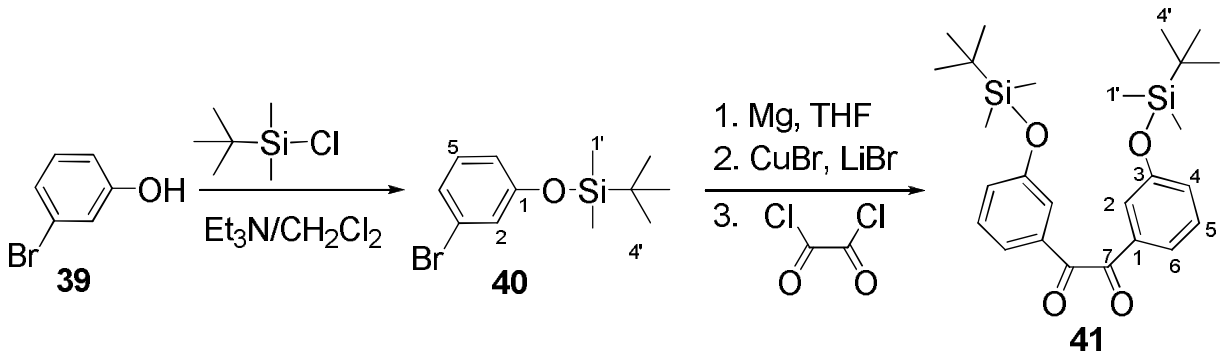

Scheme 8. Synthesis of 1,2-bis(3-(*tert*-butyldimethylsilyloxy)phenyl)ethane-1,2-dione

The ^{1}H-NMR spectrum of **40** (Table 1) revealed three proton resonances in the aromatic region and two signals in the aliphatic region. The two-proton multiplet signal at δ 7.28 is due to H-2 and H-4. The remaining one-proton multiplet signals at δ 7.09 and 6.79 correspond to H-5 and H-6, respectively. In the aliphatic region, the singlet peak at δ 1.16, which integrated for nine protons, can be assigned to H-4'. The other six-proton singlet signal at δ 0.24 is due to the methyl groups directly attached to the silicon atom.

The ^{13}C-NMR spectrum of **40** (Table 2) displayed nine carbon resonances, of which six are in the aromatic region and three are in the aliphatic region. The DEPT-135 spectrum showed four methine carbon signals in the aromatic region and two methyl carbon in the aliphatic region. The most deshielded carbon resonance can be attributed to the aromatic carbon attached directly to the oxygen atom (C-1) since the electron withdrawing inductive effect of the oxygen atom makes it highly electron deficient. On the other hand the most shielded carbon resonance in the aromatic region can be assigned to the carbon directly attached to the bromine atom because of the heavy atom effect of bromine atom. This is also confirmed by the disappearance of the corresponding peaks in the DEPT spectrum. In the aliphatic region, the peak at δ -4.4 is due to the methyl carbons attached directly to the silicon whose unusual chemical shift value (up filed) is the result of low electronegativity of silicon atom. The other signal at δ 25.4 is due to the remaining methyl carbon (C-4'). The only quaternary carbon in the aliphatic region is the peak at δ 18.2 which is attributed to C-3'. In general, the NMR results are in agreement with the structure of compound **40**.

The ^{1}H-NMR spectrum of compound **41** (Table 1) showed the presence of six different proton environments, of which four are in the aromatic region and two are in the aliphatic region. The doublet of doublets peak at δ 7.51 integrating for two hydrogens corresponds to H-2. The J values of 1.6 and 1.2 Hz are due to *meta* couplings with H-4 and H-6, respectively. The doublet of triplet at δ 7.40 is arising from H-4. The three coupling constants (J = 8, 2, 1.6) are due to *ortho* couplings with H-5, *meta* coupling with H-6 and H-2, respectively. The triplet signal at δ 7.38 can be attributed to H-5. The J values of 8 and 7.6 Hz are consequences of *ortho* couplings with H-4 and H-6, respectively. The two-proton signal at δ 7.15 is due to H-6. The three coupling constant values confirm *ortho* coupling with H-5 (J = 7.6 Hz) and *meta* couplings with H-4 (J = 2) and H-2 (J = 1.2 Hz). In the aliphatic region, the singlet signal at δ 1.01 can be attributed to the chemically equivalent twelve protons on the carbons attached to the silicones (H-1'). The remaining singlet signal at δ 0.23 integrated for eighteen protons and is accounted to the methyl protons of the *tert*-butyl groups.

The ^{13}C-NMR and DEPT-135 spectra of compound **41** (Appendices 5 and 6) displayed ten carbon signals of which four are due to quaternary carbons, four are due to methine carbons, and two are due to a methyl carbons. The signals at δ 194.6, 156.2, 134.2, 18.2, are due to quaternary carbons corresponding to the carbonyl carbons, C-1 and C-3 of the benzene ring, respectively, as confirmed by the absence of peaks in the DEPT-135 spectrum. The other resonance signals at δ 130.1, 127.0, 123.5, and 120.2 correspond to C-5, C-6, C-4, and C-2, respectively. In the aliphatic region, the carbon signals at δ 25.6, 18.2, and • 4.4 can be assigned to C-4', C-3', C-1' of the *tert*-butyldimethylsilyl groups. The data obtained from ^{1}H-NMR, ^{13}C-NMR and DEPT-135 agree with the structure of compound **41**

Table 1: ^{1}H-NMR ($CDCl_3$, 400 MHz) data (δ ppm) of compounds **40** and **41.**

40	**41**
7.28	7.51
(2H, *m*, H-2,H-4)	(2H, *dd*, *J* = 1.6, 1.2 Hz, H-2)
7.09	7.40
(1H, *m*, H-5)	(2H, *dt* , *J* = 8.0, 2.0, 1.6 Hz, H-4)
6.79	7.38
(1H, *m*, H-6)	(2H, *t*, *J* = 8.0, 7.6 Hz, H-5)
1.16	7.15
(1H, *s*, H-4')	(2H, *ddd*, *J* = 7.6, 2.0, 1.2 Hz, H-6)
0.24	1.01
(1H, *s*, H-1')	(18H, *s*, H-4')
	0.23
	(12H, *s*, H-1')

Table 2: ^{13}C-NMR (100.6 MHz, $CDCl_3$) data (δ ppm) of compounds **40** and **41**

Carbon	**40**	**41**
7	-	194.6
1	156.5	156.2
3	123.5	134.2
5	130.5	130.1
6	118.9	127.0
4	124.5	123.4
2	122.5	120.3
4'	25.6	25.6
3'	18.2	18.2
1'	-4.4	-4.4

4.1.1.1. 5,8-Bis(5-bromothiophen-2-yl)-2,3-bis(3-(*tert*-butyldimethyl-silyloxy)phenyl)quinoxaline (48)

The synthesis of the first donor-acceptor-donor segment began by bromination of 2,1,3-benzothiadiazole (**42**) (Scheme 9). Thus, treatment of **42** with Br_2 and aqueous HBr (48%) under reflux gave 4,7-dibromobenzo[*c*][1,2,5]thiadiazole (**43**) as a gray solid. The crude product was recrystallized from acetone to give compound **43** in a pure form (66.7%) as revealed by its ^{1}H- and ^{13}C-NMR spectra.

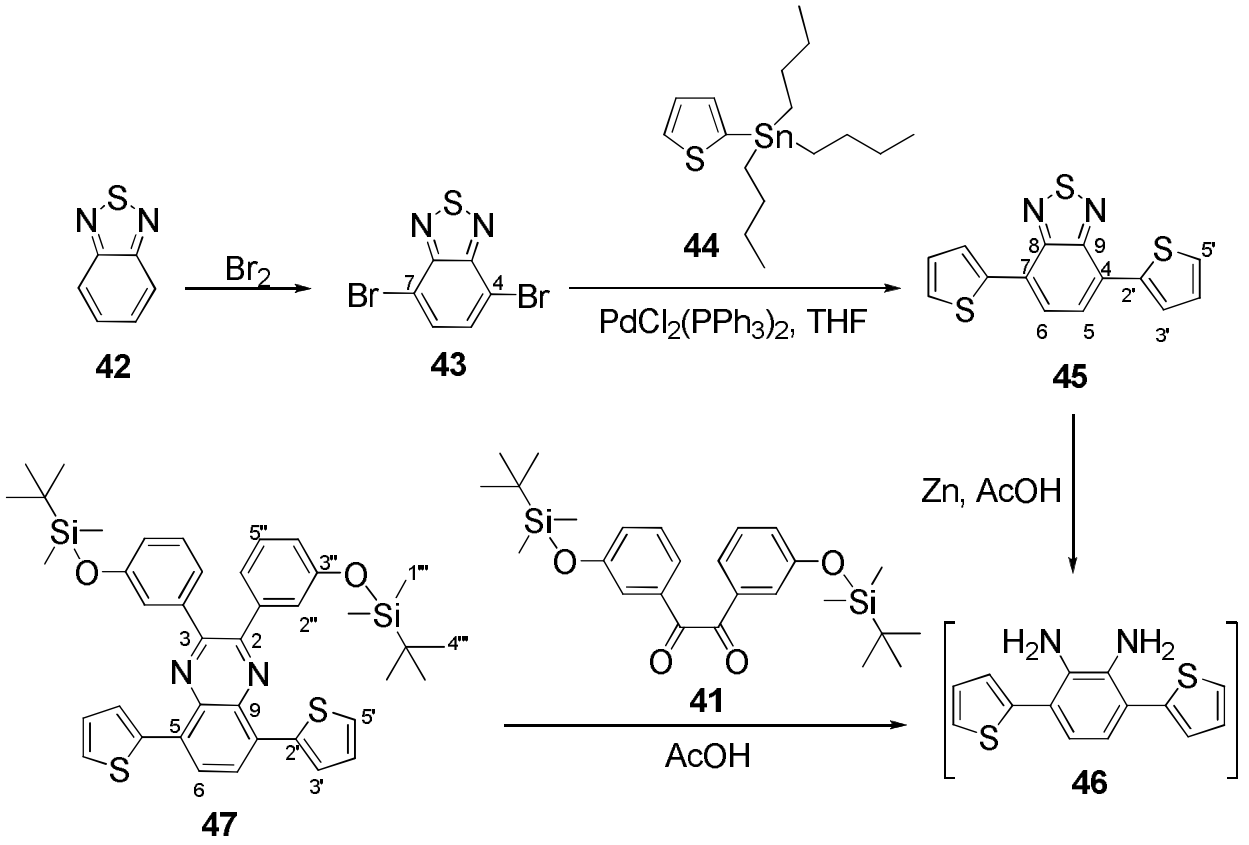

Scheme 9. Synthesis of compound **47**.

Compound **43** was subjected to Stille coupling reaction with tributyl(thiophen-2-yl)stannane (**44**) in the presence of bis-(triphenylphosphine)palladium(II) dichloride as a catalyst to form compound **45** in 78.5 % yield. Subsequent reduction of 4,7-di(thiophen-2-yl)benzo-1,2,5-thiadiazole (**45**) was accomplished by reacting with zinc dust in acetic acid heated to 80 ^{o}C for five hours (Scheme 9). The insoluble zinc-containing compound

was then removed by suction filtration and to the filtrate was added 1,2-bis(3-(*tert*-butyldimethylsilyloxy)phenyl)ethane-1,2-dione (**41**). This reaction was done by heating the mixture at 60 ^{o}C for five hours. The acetic acid was removed by rotary evaporation and the resulting orange solid mixture was dissolved in dichloromethane and washed with distilled water to afford 2,3-bis[3-(*tert*-butyldimethylsilanyloxy)phenyl]-5,8-di(thiophen-2-yl)quinoxaline (**47**) in 93.7% yield (Scheme 9). The identities of compounds **45** and **47** were confirmed by their spectroscopic data as described below.

The ^{1}H-NMR spectrum of compound **45** showed four signals in the aromatic region. The downfield doublet of doublets at δ 8.15 (*J* = 1.2, 4 Hz) integrating for two hydrogens corresponding to H-5'. The two-proton singlet centered at δ 7.91 is due to H-5 and H-6, which do not couple with each other on account of being chemically equivalent. The two proton doublet of doublets at δ 7.49 (*J* = 1.2, 5.2 Hz) correspond to H-4'. The remaining two proton doublet of doublets at δ 7.23 (*J* = 4, 5.2 Hz) is due to H-3'.

The ^{13}C-NMR spectrum of compound **45** (Appendix 8) revealed seven peaks in the aromatic region. The DEPT-135 spectrum confirmed that four of the seven carbon resonances in the aromatic region are due to methine carbon atoms. These signals appeared at δ 128.1, 127.5, 126.9 and 125.8 and correspond to C-5 and C-6, C-4', C-3', and C-5', respectively. The remaining three carbon signals at δ 152.8, 139.8, and 126.0 can then be accounted for the quaternary carbon atoms C-8 and C-9, C-2' and C-4 and C-7, respectively, each peak representing a pair of chemically equivalent carbons.

The ^{1}H-NMR spectrum of compound **47** (Table 3) showed six peaks in the aromatic region and two peaks in the aliphatic region. The most downfield singlet at δ 8.17, which integrated for two protons, can be assigned for the two chemically equivalent protons (H-5, H-6) of the quinoxaline moiety. The six-proton doublet of doublets at δ 7.92, 7.52 and 7.19 are due to the thiophene ring protons H-5', H-3', and H-4', respectively. The six-proton multiplet peaks in the range of δ 7.35-7.21 can be attributed to the methine protons of the benzene ring (H-4'', H-5'', H-6''). The other multiplet peaks in the range of

δ 6.90-6.87 can be assigned for the remaining methine proton of the benzene ring (H-2''). The aliphatic proton resonances appeared at δ 0.19 and 1.01.

Table 3: ^{1}H-NMR ($CDCl_3$, 400 MHz) data (δ ppm) of compounds **47** and **48**

47	**48**
8.17	8.09
(2H, *s*, H-6,H-7)	(2H, *s*, H-6,H-7)
7.92	7.59
(2H, *dd*, *J* = 1.2, 4 Hz, H-5')	(2H, *d*, *J* = 4 Hz H-4')
7.52	7.28-7.21
(2H, *dd*, *J* = 1.2, 5.1 Hz, H-3')	(6H, *m*, H-4'', H-5'', H-6'')
7.35-7.21	7.14
(6H, *m*, H-4'', H-5'', H-6'')	(2H, *d*, *J* = 4 Hz, H-3')
7.19	6.91
(2H, *dd*, *J* = 4, 5.1 Hz, H-4')	(2H, *m*, H-2'')
6.90-6.87	1.03
(2H, *m*, H-2'')	(18H, *s*, H-4''')
1.01	0.21
(18H, *s*, H-4''')	(12H, *s*, H-1''')
0.19	
(12, *s* H-1''')	

The ^{13}C-NMR spectrum of compound **47** (Table 4, Appendix 11) revealed fourteen carbon resonances above δ 100 and three carbon signals below δ 100. Of the fourteen carbon signals in the aromatic region, eight are methine carbons and the remaining six resonances represent the quaternary carbons as indicated by the DEPT-135 spectrum. The most deshielded carbon resonance can be attributed to the aromatic carbons attached directly to the oxygen atoms since the electron withdrawing inductive effect of the oxygen atom makes them highly electron deficient. The three carbon signals in the aliphatic region, of which two are methyl carbon peaks (C-1''', C-4'''') and one is quaternary carbon peak (C-3''), can be assigned for the carbon atoms of the *tert*-

butyldimethylsilyl group. Both the ^{1}H- and ^{13}C-NMR data discussed above agree very well with the structure of the compound.

Table 4: ^{13}C-NMR (100.6 MHz, $CDCl_3$) data (δ ppm) of compounds **47** and **48**

Carbon	**47**	**48**
C-3''	155.7	155.8
C-2, C-3	151.5	152.1
C-9,C-10	140.1	139.6
C-2'	138.8	139.6
C-5, C-8	137.1	136.5
C-1''	131.2	130.7
C-5''	129.3	129.2
C-6, C-7	128.7	125.8
C-4'	127.1	129.4
C-3'	126.7	125.7
C-5'	126.5	117.1
C-6''	123.6	123.6
C-4''	121.8	121.7
C-2''	121.1	121.2
C-4'''	25.7	25.7
C-3'''	18.2	18.2
C-1'''	-4.3	-4.2

The last step in the synthesis of the first donor-acceptor-donor monomer **48** involved bromination of compound **47.** Thus, compound **47** was dibrominated using NBS in THF to afford 5,8-bis(5-bromothiophen-2-yl)-2,3-bis(3-(*tert*-butyldimethylsilyloxy)phenyl)quinoxaline (**48**) (Scheme 10).

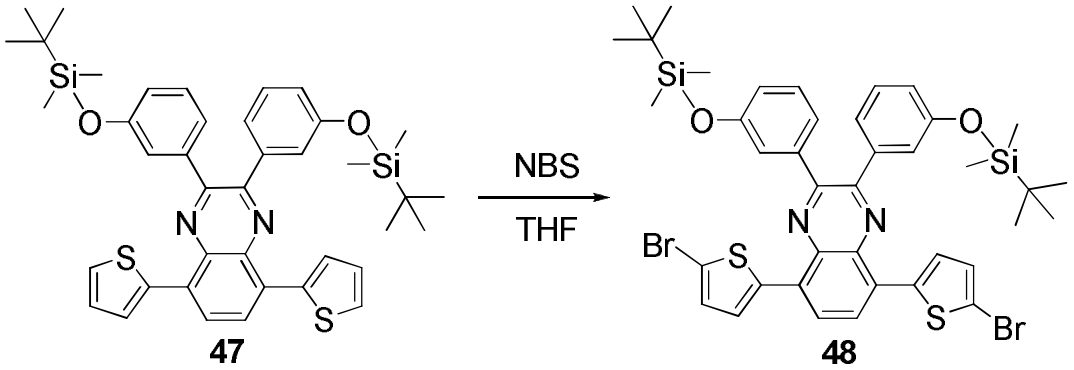

Scheme 10. Bromination of 2,3-bis(3-(*tert*-butyldimethylsilyloxy)phenyl)-5,8-di-(thiophen-2-yl)quinoxaline (**47**)

The ^{1}H-NMR of spectrum of compound **48** (Table 3) showed the presence of five aromatic proton resonances and two aliphatic proton signals in the up field region. The singlet at δ 8.09 is due to chemically equivalent protons H-6 and H-7. The doublet signal at δ 7.59 is attributed to H-4'.The multiplet signals in the range of δ 7.28-7.21, which integrated for six protons are assigned to the methine protons of the benzene ring (H-4'', H-5'', H-6''). The remaining doublet signal at δ 7.14 corresponds to H-3'. The unresolved multiplet signal centered at δ 6.19 can be attributed to H-2''. The singlet peaks at δ 1.03 and 0.21 can be assigned to methyl protons (H-4''', H-1''') in the aliphatic region.

The ^{13}C-NMR spectrum of compound **48** (Table 4) displayed sixteen carbon resonances, of which, thirteen appeared in the aromatic and the remaining three appeared in the aliphatic region. The DEPT-135 spectrum revealed seven methine and two methyl carbon resonances. The remaining seven carbon resonances are quaternary carbons of which two quaternary carbon resonances (C-2' and C-9, C-10) appeared together at δ 139.6. The most shielded carbon resonance in the aromatic region can be attributed to the carbons directly attached to the bromine atoms since the heavy atom effect of the bromine atoms makes them electron rich.

4.1.2. 5,8-Bis(5-bromothiophen-2-yl)-2,3-bis(3-(2-(2-methoxy-ethoxy)ethoxy)phenyl)quinoxaline (**50**)

The second donor-acceptor-donor segment **50** was prepared starting from 5,8-bis(5-bromothiophen-2-yl)-2,3-bis(3-(*tert*-butyldimethylsilyloxy)phenyl) quinoxaline (**48**) as shown in Scheme 11. Removal of the *t*-butyldimethylsilyl groups from **48** by reaction with tetra-*n*-butylammonium fluoride afforded 3,3'-(5,8-bis(5-bromothiophen-2-yl)quinoxaline-2,3-diyl)diphenol (**49**) in 60.2 % yield.

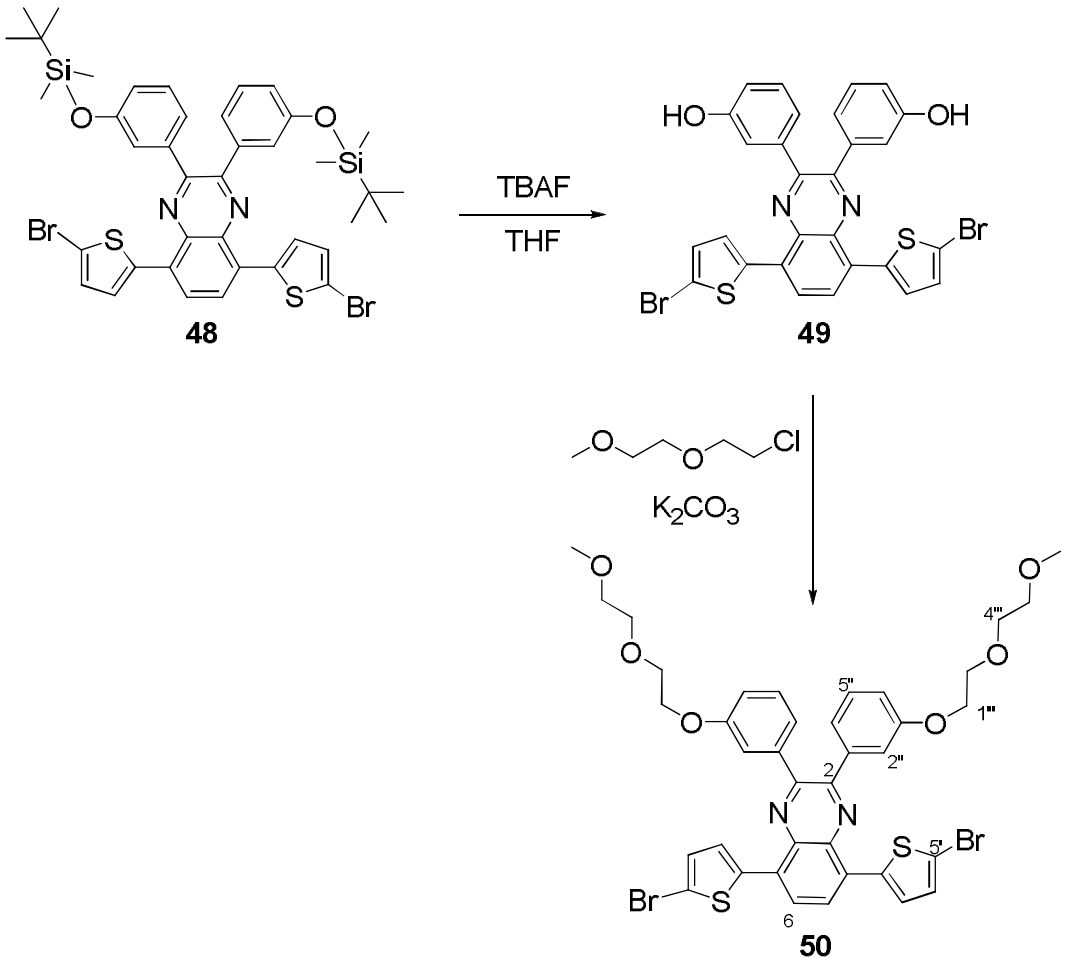

Scheme 11. Synthesis of 5,8-bis(5-bromothiophen-2-yl)-2,3-bis(3-(2-(2-methoxy-ethoxy)ethoxy)phenyl)quinoxaline (**50**)

The ^{1}H-NMR spectrum of **49** (Table 5) showed five peaks in the aromatic region, which integrated for a total of 16 protons. The appearance of the spectrum is almost similar to the ^{1}H-NMR spectrum of compound **48** except for the presence of an additional phenolic protons peak in the range of δ 7.28-7.19 as a result of loss of the *tert*-butyldimethylsilyl group. The other signals can be analyzed in the same way as described above for compound **48**.

The ^{13}C-NMR spectrum of compound **49** (Table 6) displayed the existence of thirteen carbon resonances in the aromatic region. The appearance of the spectrum is similar to that of the ^{13}C-NMR spectrum of compound **48** except for the disappearance of two methyl and one quaternary carbon resonances in the aliphatic region because of the removal of the silyl protecting groups. The ^{1}H-NMR, ^{13}C-NMR and DEPT-135 spectral data agree very well with the structure of the compound **48**.

In the subsequent step, 5,8-bis(5-bromothiophen-2-yl)-2,3-bis(3-(2-(2-methoxyethoxy)-ethoxy)phenyl)quinoxaline (**50**) was synthesized as red solid by alkylation reaction of **49** as shown in Scheme 11. Compound **50** was obtained in 79.68% yield after overnight refluxing of a mixture of compound **49**, 1-chloro-2-(2-methoxyethoxy)ethane and potassium carbonate in DMF at 100^{o}C.

The ^{1}H-NMR spectrum of compound **50** revealed five signals in the aromatic region and five signals in the aliphatic region, which integrated for a total of 36 protons. The two-proton singlet peak at δ 7.75 can be ascribed to the pair of chemically equivalent protons of the quinoxaline moiety (H-6, H-7). The broad peak at δ 7.53 is due to H-2''. The doublet peak at δ 7.32 is due to H-4'. The triplet signal at δ 7.22 can be assigned to H-5''. The multiplet signal at δ 7.04 corresponds to H-6'', H-4'' and H-3'. In the aliphatic region, the first two triplet peaks at δ 4.24 and 3.94 are attributed to the methylene protons (H-1''', H-2'') . The remaining two triplets at δ 3.77 and 3.62 are due to H-4''' and H-5''', respectively. The signal due to the methyl protons appeared at δ 3.43 as singlet.

Table 5: ^{1}H-NMR ($CDCl_3$, 400 MHz) data (δ ppm) of compounds **49** and **50**

49	**50**
8.07	7.75
(2H, *s*, H-6,H-7)	(2H, *s*, H-6, H-7)
7.58	7.53
(2H, *d*, *J* = 4.4 Hz, H-4')	(2H, *s*, H-2'')
7.28-7.19	7.32
(8H, *m*, H-4'', H-5'', H-6'', H-1''')	(2H, *d* ,*J* = 4 Hz, H-4')
7.13	7.22
(2H, *d*, *J* = 4 HZ, H-3')	(2H, *t*, *J* = 7.8, Hz, H-5'')
6.96	7.04
(2H, *m*, H-2'')	(6H, *m*, H-6'', H-4'', H-3')
	4.24
	(4H, *t*, *J* = 8.8 Hz, H-1''')
	3.94
	(4H, *t*, *J* = 8.8 Hz, H-2''')
	3.77
	(4H, *t*, *J* = 9.2 Hz, H-4'')
	3.62
	(4H, *t*, *J* = 9.2 Hz, H-5''')
	3.43
	(6H, *s*, H-7'')

The ^{13}C-NMR spectrum of **50** displayed the presence of 19 carbon resonances, of which fourteen are in the aromatic region and the remaining five are in the aliphatic region. The DEPT-135 spectrum showed seven methine carbon signals in the aromatic region, and four methylene and one methyl carbon resonances in the aliphatic region. Out of the seven methine carbon signals, four are due to the benzene-ring methine carbons (C-5'', C-4'', C-6'', C-2''), one signal is due to methine carbon of the quinoxaline unit and the remaining two signals are due to the methine carbons of thiophene rings

(C-3', C-4'). The peaks at δ 72.0, 70.8, 69.8, 67.8 and 59.1 correspond to the carbon atoms 5''', 4''', 2''', 1''' and 7''', respectively.

Table 6: ^{13}C-NMR (100.6 MHz, $CDCl_3$) data (δ ppm) of compounds **49** and **50**

Carbon	**49**	**50**
C-3''	155..8	159.0
C-2, C-3	151.8	151.3
C-9,C-10	139.6	139.3
C-2'	139.6	139.1
C-5, C-8	136.6	136.0
C-1''	130.6	130.0
C-5''	129.5	129.1
C-6, C-7	129.2	128.9
C-4'	125.8	125.3
C-3'	125.7	125.2
C-4''	122.8	123.3
C-6''	117.2	117.5
C-5'	117.1	117.1
C-2''	116.5	115.0
5'''	-	72.0
4'''	-	70.8
2'''	-	69.8
1'''	-	67.8
7'''	-	59.1

4.2. Synthesis of Fluorene-Based Alternating Copolymers

Quinoxaline-based copolymers are preferred due to their good charge-transfer characteristics and stability for device applications [22]. In particular, fluorene-quinoxaline alternating copolymers have been highly studied since they exhibited high

power conversion photovoltaic efficiency due to their balanced electron and hole mobilities [35]. In the course of this work, two alternating polyfluorene copolymers were synthesized. The discussion that follows describes the syntheses of these polymers.

4.2.1. Preparation of Polymers 52 and 54

Once the quinoxaline-based segments were prepared, the last step in the synthesis of the fluorene-based alternating copolymers **52** and **54** involved Suzuki polymerization reactions of the dibromides described above with boronate esters **51** and **53.** Thus, copolymer **52** was derived from the reaction of dibromide **50** and 2-(9,9-bis(2-(2-methoxyethoxy)ethyl)-7-(4,4,5,5-tetramethyl-1,3,2-dioxaborolan-2-yl)-9H-fluoren-2-yl)-4,4,5,5-tetramethyl-1,3,2-dioxaborolane (**51**) in the presence of tetrakis-(triphenylphsphine)Pd(0) as shown in Scheme 12. Similarly, the second alternating copolymer **54** was obtained from Suzuki coupling reaction between 50% monomer **53**, 10% monomer **48** and 40% monomer **50** (Scheme 13).

Suzuki coupling methodology was employed for polymerization since it is tolerant of a large variety of functional groups, insensitive to the presence of water, and easy to make high molecular weight polymers [46]. The boronate esters **51** and **53** used in this work were previously synthesized in our laboratory by Yadessa M. [45] and Desta G. , respectively. The synthesis of boronate ester **53** is as described in the experimental section. To increase the stability of the polymers, end-capping reactions were performed using bromobenzene and phenyl boric acid. The low molecular weight polymers were isolated by Soxhlet extraction with diethyl ether and the chloroform-soluble materials were precipitated from methanol. Both polymers were obtained as brown solid. The chloroform solutions of the polymers had deep-red colors.

Polyfluorene derivatives containing ethylene oxide side groups were used as electron injecting layers in PLEDs. The electroluminescence (EL) efficiency of such polymers was significantly enhanced as compared to polymers which lack ethylene oxide groups

because of ion transporting properties of the ethylene oxide groups leading to large space charge [47]. It has been reported that because ethylene oxide groups were able to transport mobile ion, poly(ethylene oxide) could be used as a solid-state ionic transporting material in light emitting electrochemical cells (LECs) [48,49]. Monomers containing polar side groups are also used to improve the miscibility of the polymer with fullerene and stabilize the morphology [36].

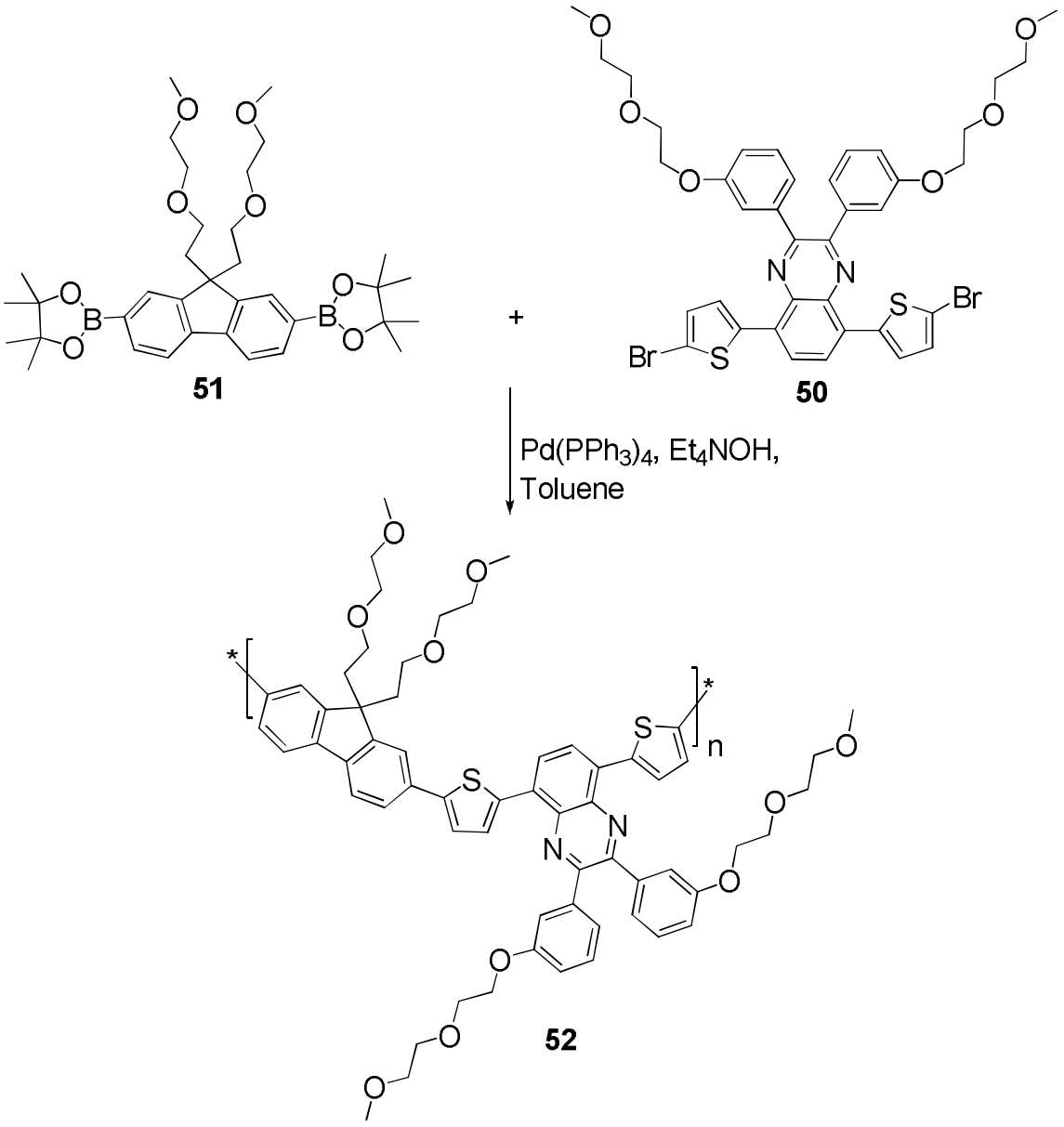

Scheme 12. Synthesis of polymer **52** through Suzuki polymerization reaction**.**

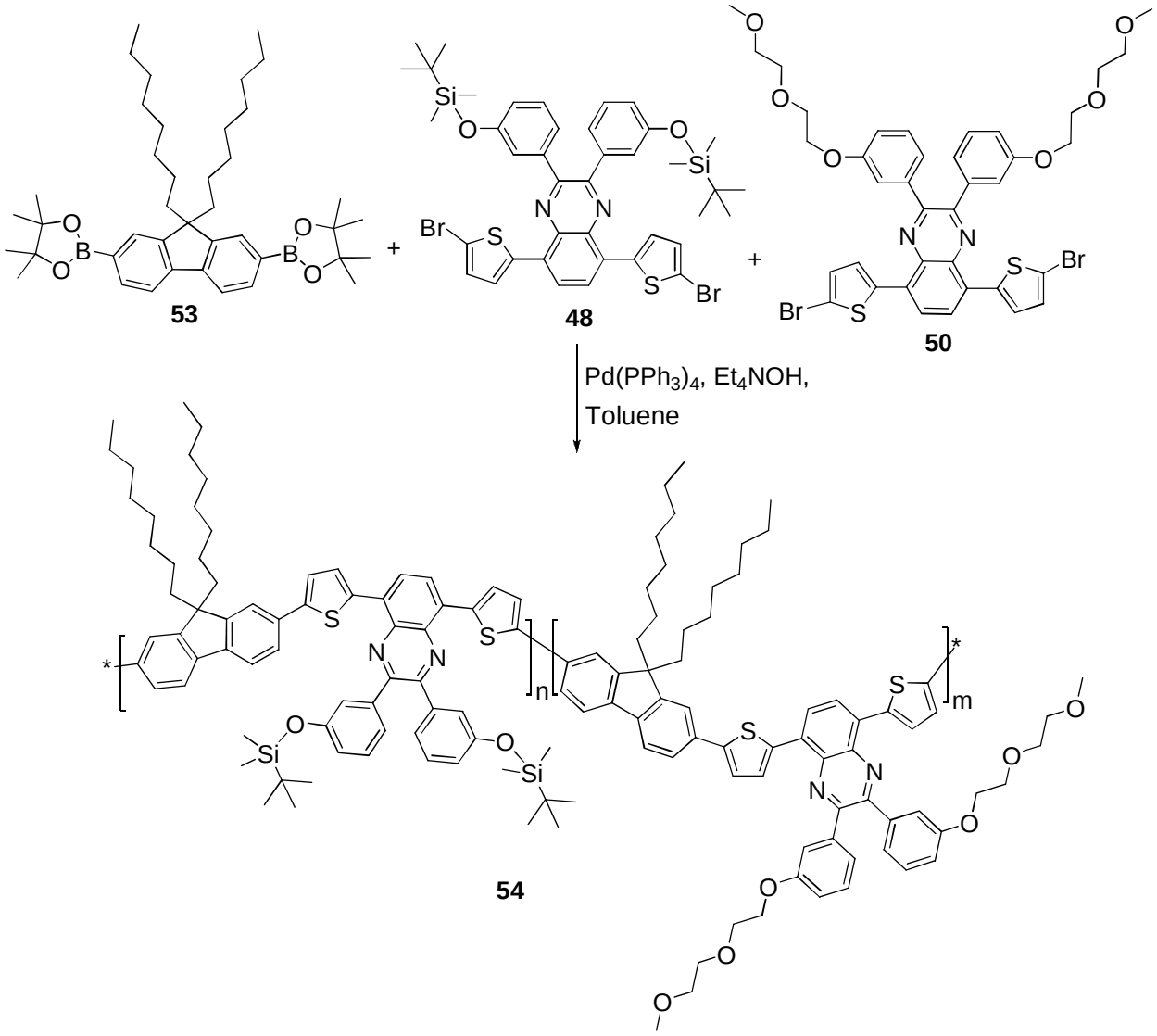

Scheme 13. Synthesis of copolymer **54** through Suzuki polymerization reaction.

4.2.2. Attempted Synthesis of Copolymer 55

Attempt was also made to prepare poly[3-(5-(5-((7-(5-(2,3-bis(3-(2-(2-methoxyethoxy)ethoxy)phenyl)-8-(thiophen-2-yl)quinoxalin-5-yl)thiophen-2-yl)-9,9-dioctyl-9H-fluren-2yl)methyl)thiophen-2-yl)-8-(5-(9,9-diocthyl-9H-fluoren-2-yl)thiophen-2-yl)-3-(3-hydroxyphenyl)quinoxalin-2-yl)phenol] (**55**) by the reaction between copolymer **54** and tetrabutylammonium fluoride as shown in Scheme 14. However, this attempt did not lead to the desired product as confirmed by the ^{1}H-NMR spectrum.

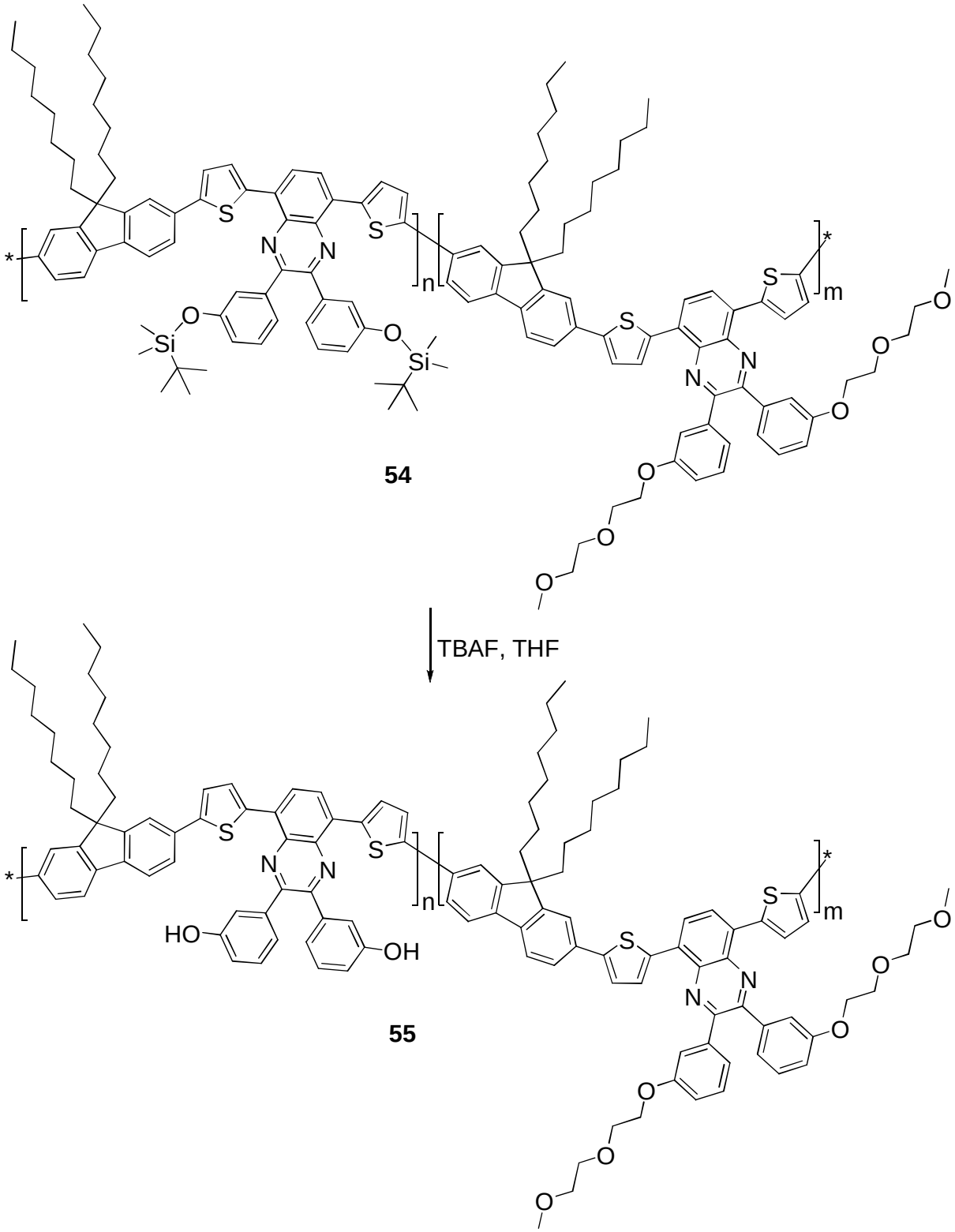

Scheme 14. Synthesis of copolymer **55**

4.2.3. Optical properties

Optical spectra of conjugated polymers provide information about the electronic structure and the character of the band-gap. Hence, it is important to study the optical properties to have more insight into the electronic structure of polymers. Optical properties of polymers were investigated both in solution and in the solid state.

The ultraviolet-visible (Uv-Vis) absorption spectra of the polymers were measured in chloroform solutions and in solid films spin-coated on glass plates. Figures 5 and 6 show UV-Vis absorption spectra of polymers **52** and **54** in chloroform solutions and thin films. The onset of absorption wavelength, both in solutions and films and the optical band-gap (E_g^{opt}) values calculated from the onset of absorption are summarized in Table 7.

It can be seen from Figure 6 and 7 that there are two absorption peaks for the polymers in chloroform solutions as well as in films. These ‘’camel-back’’ absorption spectra are characteristic of introduction of donor-acceptor unit on to the polyfluorene backbone and are different from the single broad absorption peak observed in traditional π-conjugated polymers such as neat polyfluorene. Based on previous studies carried out on similar PF copolymers with donor-acceptor-donor moieties, the red band of the absorption spectrum is ascribed to a localized transition between the donor-acceptor-donor charge transfer states and the blue band is identified as excitonic π–π* transition [35,50]. Compared to the corresponding values of polymer **52,** the short-wavelength absorption maximum in the Uv-Vis spectrum of the $CHCl_3$-solution of polymer **54** is blue-shifted by 6 nm and the long-wavelength absorption maximum is red-shifted by 3 nm, due to the presence of ethylene oxide side groups instead of octyl side groups in polymer **52**.

As compared to the Uv-Vis spectra in $CHCl_3$ solution, the spectra of the thin films of both polymer **52** and **54** revealed that the long-wavelength absorption maxima are red-shifted by about 20 nm and 12 nm, respectively. Similarly, the short-wavelength absorption maxima are red-shifted by 5 nm and 8 nm, respectively (Table 7). In

addition, broadening of peak shape was observed in the spectra of the thin films of both polymers. This suggests that the polymer chains are close enough in the film state to facilitate interchain energy transfer from fluorene segments to the lower band-gap co-monomer units. The solid state generally favors the formation of aggregates which benefits the polymer backbone in more planar conformation, which extends the conjugation length of the π electrons. The more homogeneity of the polymer in the solution form leads to narrower absorption bands [51].

Table 7: Optical properties of the polymers

Polymer	λ_{max} (nm)		λ_{onset}(nm)		E_g^{opt} (eV)
	Solution	Film	Solution	Film	
52	392, 519	397, 539	636	714	1.74
54	386, 522	394, 534	640	683	1.82

The absorption spectra of copolymers **52** and **54** are much more red shifted than poly(quinoxaline) [9], polythiophene [9], and polyfluorene [37] . This suggests the significance of the intramolecular charge transfer between the donor and quinoxaline moieties.

The absorption onsets of polymer **52** and **54** are red-shifted compared to the reported values of **APFO-15** (**35**) and **APFO-25** (**36**) [35, 36]. These results indicate that the presence of the ethylene oxide side chains in **52** and **54** plays an important role to change the optical properties of the polymers.

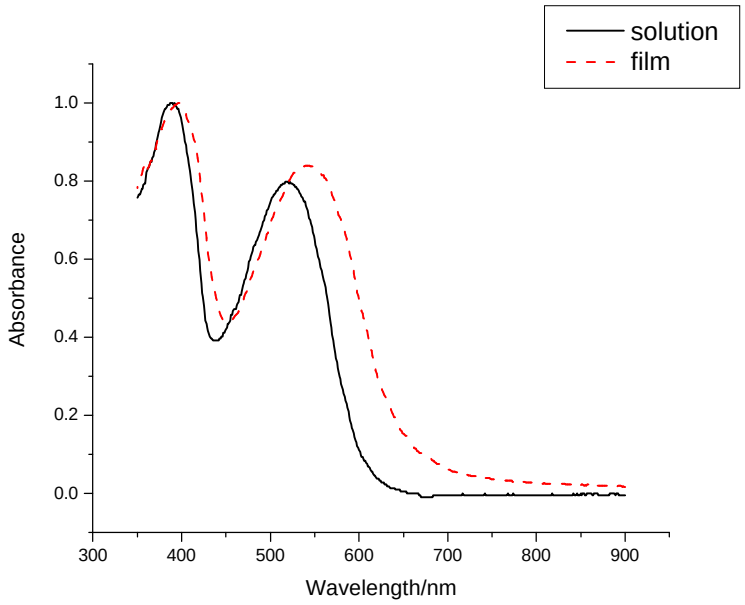

Figure 6. Uv-Vis absorption spectrum of **52** in $CHCl_3$ solution (solid curve) and in thin film (dashed curve).

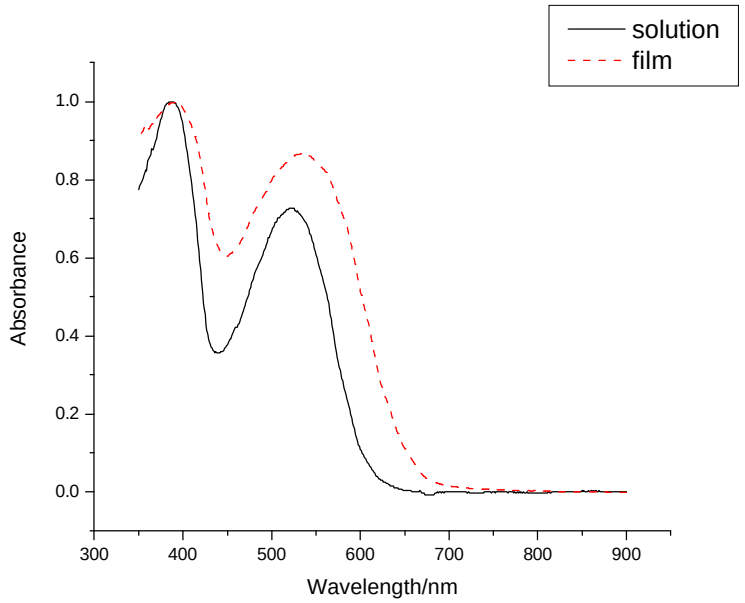

Figure 7. Uv-Vis absorption spectrum of **54** in $CHCl_3$ solution (solid curve) and in thin film (dashed curve).

4.2.4. Electrochemical properties

Cyclic voltammetry is a method that is frequently employed to simultaneously evaluate both the HOMO and LUMO energy levels and the band-gap of a polymer [51]. The oxidation process corresponds to the removal of charge from the HOMO band, whereas the reduction cycle corresponds to the filling of the energy state by electrons to the LUMO band. Therefore, the oxidation and reduction potentials are closely related to the energies of the HOMO and LUMO levels of an organic molecule and thus can provide important information regarding the magnitude of the energy gap [51]. The electrochemical properties and the HOMO and LUMO levels of polymers **52** and **54** were investigated by cyclic voltammetry.

Figures 7 and 8 show the cyclic voltammograms of **52** and **54**, respectively. Based on the electrochemical results, the ionization potential (HOMO) and electron affinity (LUMO) were calculated from the onset potentials of oxidation ($E_{O,\ ox}$) and reduction ($E_{O,red}$), respectively, on the basis of the reference energy level according to Equations 1 and 2. The electrochemically determined band-gaps (E_g^{ec}) were deduced from the difference between onset potentials from oxidation and reduction of polymers as depicted in Equation 3 [51, 52].

$$HOMO = -(E_{O,\ ox} + 4.39)\ (eV) \quad (1)$$

$$LUMO = -(E_{O,\ red} + 4.39)\ (eV) \quad (2)$$

$$E_g^{ec} = E_{O,\ ox} - E_{O,\ red} \quad (3)$$

The onset potentials were determined from the intersection of the two tangents drawn at the rising current and baseline charging current of the CV traces. The polymer films coated on a glassy carbon working electrode, supported in 0.10 M *tetra-n* butylammonium perchlorate (Bu_4NClO_4) in anhydrous acetonitrile, were measured at a scanning rate of 100 mV/s.

In the oxidation scan, the oxidation potentials (p-doping) of polymers **52** (Figure 8) and **54** (Figure 9) occur at 1.11 and 1.07 eV, which correspond to HOMO energy levels of -5.5 eV and -5.46 eV, respectively. In the reduction scan, the reduction potentials (n-doping) of polymers **52** and **54** occur at -1.09 and -1.11 eV, which correspond to LUMO energy levels of -3.3 and -3.28 eV, respectively. The electrochemical band-gaps of polymers **52** and **54,** calculated from the oxidation and reduction potentials according to Equation 3, are 2.2 and 2.18 eV, respectively.

Note that the band-gaps calculated from the UV–Vis absorption onset and the cyclic voltammogram are different. The cyclic voltammetry data are more substantial than the optical data from Uv–Vis absorption onset [51].

The electrochemical and optical band-gap of copolymer **52** are lower than that of **APFO-15** (**35**), which is due to the presence ethylene oxide side groups in the copolymer. Compared to copolymer **54**, the optical and electrochemical band-gaps of **APFO-25** are higher. This difference can be attributed to the existence of ethylene oxide side chains in the quinoxaline unit of the copolymer **54**.

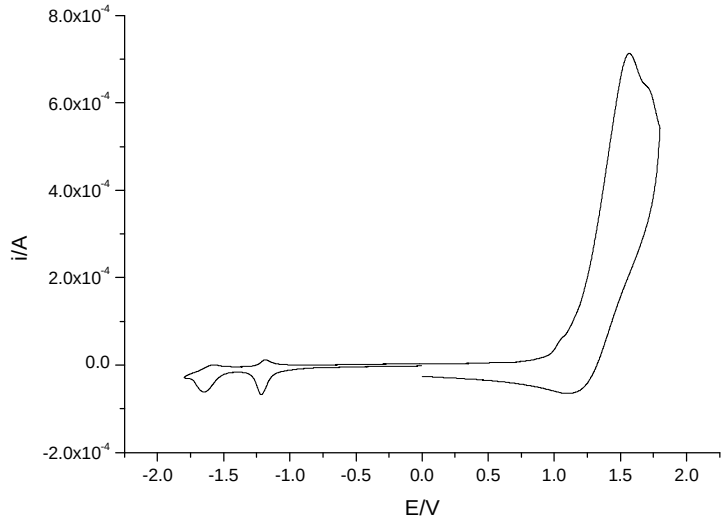

Figure 8. Cyclic voltammogram for copolymer **52.**

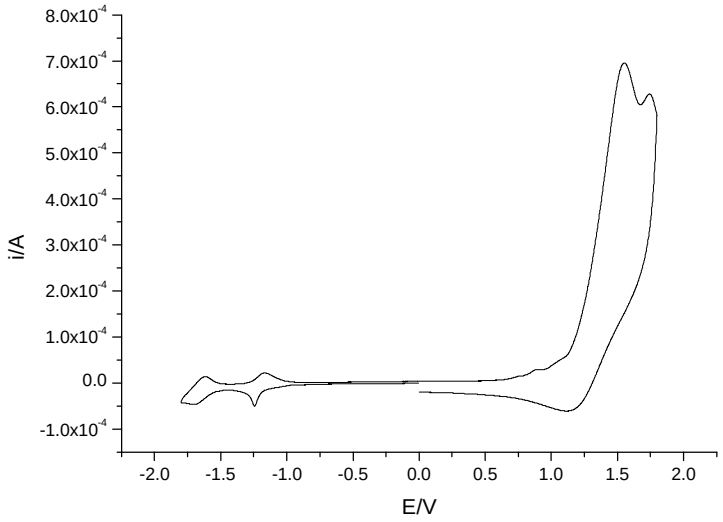

Figure 9. Cyclic voltammogram for copolymer **54**

5. CONCLUSION

Donor-acceptor copolymers have attracted significant scientific interest recently as their electronic and optoelectronic properties can be manipulated through intramolecular charge transfer and due to their potential applications in various organic electronic devices. In this project work, two fluorene-based copolymers containing donor-acceptor-donor segment were synthesized. The polymerization reactions were conducted by Suzuki coupling reactions using Pd(0) as a catalyst and tetraethylammonium hydroxide as a base. The resulting polymers exhibited good solubility in chloroform and their colors in chloroform were deep-red. The optical band-gaps for polymers **52** and **54** were estimated to be 1.74 and 1.82 eV, respectively, .from their Uv-Vis absorption spectra. On the other hand, the electrochemical energy band-gaps for **52** and **54** were found to be 2.2 and 2.18 eV, respectively. Further investigation on physical properties such as molecular weight determination, FTIR studies, electroluminescence properties etc., is necessary to fully characterize the polymers.

6. EXPERIMENTAL

6.1. Materials and Methods

^{1}H-NMR and ^{13}C-NMR spectra were recorded on a Bruker Avance 400 MHz spectrometer at 400.13 and 100.6 MHz, respectively in $CDCl_3$ and chemical shifts were reported in $\bullet_{ppm}$ unit. Cyclic voltammograms (CVs) were recorded on a BASi Epsilon-EC potentiostat using platinum electrodes at a scan rate of 100 $mV.s^{-1}$ and a Ag/Ag^{+} (0.10 M of $AgNO_3$ in acetonitrile) reference electrode in solution of 0.1 M of tetrabutylammonium tetrachloroborate (Bu_4NBCl_4) in acetonitrile. UV-Vis absorption spectra were recorded using T60 UV-Vis spectrophotometer.

6.2. Reagents

NBS, anhydrous Na_2SO_4, ethyl acetate, 2-(tributylstannyl)thiophene, 3-bromophenol, $CDCl_3$, bromine, *bis*(triphenylphosphine)palladium(II) chloride, 2,1,3-benzothiadiazole, tetra-butylammonium fluoride, *t*-butyldimethylsilyl chloride, bromobenzene, phenyl boric acid, dichloromethane, oxalyl chloride, chloroform, hexane, acetone were bought from Aldrich and were used as received. Toluene used for polymerization reactions was distilled before use. Analytical grade diethyl ether, chloroform and methanol purchased from BDH were used as received. Tetrahydrofuran was dried over sodium-benzophenone under nitrogen atmosphere when moisture-free reactions needed to be conducted. Analytical thin layer chromatography (TLC) was performed on Merck silica gel F_{254} 0.2 mm precoated plates on aluminium. Visualization was accomplished by an ultraviolet lamp (254 and 365 nm). Silica gel column chromatography was carried out with silica gel (230-400 mesh).

6.3. Monomer Synthesis

6.3.1. 4,7-Dibromobenzo[*c*][1,2,5]thiadiazole (43)

In 1L round bottom flask equipped with reflux condenser and a pressure equalizing dropping funnel, a mixture of 2,1,3-benzothiadiazole (**42**) (20 g , 0.147 mol) and 48% HBr (80 mL) were heated at 110^{o}C with continuous stirring. Bromine (22 mL) was added to the mixture from a pressure equalizing funnel slowly within 30 min. A white-yellowish solid was deposited on the walls of the flask during refluxing. Additional HBr (22 mL) was added and the mixture was heated for 2 hrs. The mixture was allowed to cool to room temperate and filtered by suction. The residue was washed with sodium thiosulphate and then with water. The resulting product was recrystallized from acetone and the crystals were collected by suction filtration and allowed to dry in a vacuum oven overnight to afford compound **43** (37.4 g, 91.0%).

Mp: 175-177 ^{o}C; ^{1}H-NMR ($CDCl_3$, 400 MHz) $\bullet_{ppm}$ 7.73 (2H, *s*, H-5, H-6); ^{13}C-NMR (100.6 MHz, $CDCl_3$), $\bullet_{ppm}$: 152.94 (C-8 & C-9), 132.37 (C-5 & C-6), 113.9 (C-4 & C-7).

6.3.2. 4,7-Di(thiophen-2-yl)benzo[*c*][1,2,5]thiadiazole (45)

4,7-Dibromobenzo[*c*][1,2,5]thiadiazole (**43**) (10 g, 34 mmol) and $PdCl_2(PPh_3)_2$ (0.48 g, 0.68 mmol) were dissolved in THF (140 mL) by heating to reflux under nitrogen. Tributyl(thiophen-2- yl)stannane (20.6 mL, 68 mmol) was then added drop by drop from a pressure-equalizing dropping funnel over 70 min. The refluxing continued overnight. The reaction progress was checked by thin layer chromatography using dichloromethane:pet ether (1:4) as eluent. The mixture was cooled and the solvent was removed on a rotary evaporator and to the residue, petroleum ether was added. The solid formed was collected by suction filtration to afford **45** (8.02 g, 78.5%).

^{1}H-NMR ($CDCl_3$, 400 MHz), $\bullet_{ppm}$: 8.15 (2H, *dd*, *J* = 1.2, 4 Hz, H-5'), 7.91 (2H, *s*, H-5, H-6), 7.49 (2H, *dd*, *J* = 1.2, 5.2 Hz, H-3'), 7.23 (2H, *dd*, *J* = 4, 5.2 Hz, H-4'); ^{13}C-NMR

($CDCl_3$, 100.6 MHz), • $_{ppm}$: 152.66 (C-8, C-9), 139.37 (C-2'), 128.05 (C-5, C-6), 127.53 (C-4'), 126.85 (C-3'), 126.02 (C-4, C-7), 125.82 (C-5')

6.3.3. (3-Bromophenoxy)(*tert*-butyl)dimethylsilane (40)

3-Bromophenol (20 g, 0.12 mol) was mixed with of dichloromethane (300 mL) in a dry 1L two-necked round bottom flask equipped with a magnetic stirrer. The mixture was stirred vigorously and triethylamine (24 mL) was added. After the 3-bromophenol dissolved completely, the *tert*-butyldimethylsilyl chloride (17.42 g, 0.12 mol) was added and stirring continued overnight. The white solid precipitate was removed by suction filtration. The yellowish filtrate was washed with distilled water and dried over anhydrous Na_2SO_4. Evaporation of the solvent gave yellowish oil and checked by thin layer chromatography using hexane: toluene (1:1) mixture, which showed the presence of impurity. The crude product was then purified by washing with 5% NaOH and distilled water, dried over anhydrous Na_2SO_4 and dried overnight in vacuum oven to afford **40** as a yellowish oil (25 g, 75.3%).

^{1}H-NMR ($CDCl_3$, 400 MHz), • $_{ppm}$: 7.28 (2H, *m*, H-2, H-4), 7.09 (1H, *m*, H-6), 6.79 (1H, *m*, H-7), 1.16 (1H, *s*, H-4'), 0.24 (1H, *s*, H-1'); ^{13}C-NMR ($CDCl_3$, 100.6 MHz), • $_{ppm}$: 156.5 (C-1), 130.5 (C-5), 124.5 (C-4), 123.5 (C-3), 122.5 (C-2), 118.9 (C-6), 25.6 (C-4'), 18.2 (C-3'), -4.4 (C-1')

6.3.4. 1,2-Bis(3-(*tert*-butyldimethylsilyloxy)phenyl)ethane-1,2-dione (41)

In a three-necked round bottom flask equipped with a pressure equalizing dropping funnel and a condenser, the Grignard reagent was prepared by drop wise addition of (3-bromophenoxy)(*tert*-butyl)dimethylsilane (10.2 g, 0.04 mol) in THF (10 mL) to a suspension of magnesium (1.01 g, 0.042 mol) in THF (18 mL) . In a separate three-necked round bottom flask, a solution of LiBr (6.13 g, 0.071 mol) in THF (20 mL) was added to a stirred suspension of CuBr (5.092 g, 0.04 mol) in THF (20 mL) under nitrogen. The mixture was stirred until it became homogenous and cooled to a

temperature of -78 ^{o}C. The Grignard reagent was then added to LiBr/CuBr suspension using cannula. After 30 min, oxalyl chloride (2.464 g, 0194 mol) was quickly added using syringe. Stirring continued overnight at room temperature. The reaction mixture was quenched with saturated NH_4Cl and then extracted with diethyl ether and washed with saturated NH_4Cl. It was dried over anhydrous Na_2SO_4. Evaporation of the solvent afforded light red crude product (12.5 g). The crude product was purified by chromatography on a column of silica gel using petroleum ether:ethyl acetate (9.5:0.5) as eluent. Evaporation of the solvent afford diketone **41** (1.15 g, 6.9%).

^{1}H-NMR ($CDCl_3$, 400 MHz), • $_{ppm}$: 7.51(2H, *dd*, *J* = 1.6, 1.2 Hz, H-2), 7.40 (2H, dt, *J* = 12, 2, 1.8 Hz, H-4), 7.38 (2H, *t*, *J* = 8, 7.6 Hz, H-5), 7.15 (2H, *ddd*, *J* = 8.1, 2.6, 1.2 Hz H-6), 1.01 (18H, *s*, H-3'), 0.23 (12H, *s*, H-1'); ^{13}C-NMR ($CDCl_3$, 100.6 MHz), • $_{ppm}$: 194.6 (C=O), 156.2 (C-1), 134.2 (C-3), 130.1 (C-5), 126.96 (C-6) ,123.5 (C-4), 120.3 (C-2), 25.6 (C-3'), 18.2 (C-2'), -4.4 (C-1')

6.3.5. 2,3-Bis(3-(*tert*-butyldimethylsilanyloxy)phenyl)-5,8-di(thiophen-2-yl) quinoxaline (47)

4,7-Di(thiophen-2-yl)benzo[*c*][1,2,5]thiadiazole (**45**) (0.702 g, 2.34 mmol) and zinc (5 g, 76.53 mmol) were kept in of acetic acid (100 mL) and heated to 80 ^{o}C under nitrogen for 5 h. The zinc compound was then removed by suction filtration using a sintered glass funnel and the filtrate was transferred in to a new flask to which 1,2-bis(3-(*tert*-butyldimethylsilanyloxy)phenyl)ethane-1,2-dione (**41**) (1.1 g, 2.34 mmol) was added. The mixture was heated at 60 ^{o}C for 5 h. The acetic acid was removed by rotary evaporation and gave an orange solid residue, which was dissolved in dichloromethane, washed with distilled water and dried over anhydrous $Na_2SO_{4,.}$ Removal of the solvent by rotary evaporation afforded **47** (1.55 g, 93.71%) as an oil.

^{1}H-NMR ($CDCl_3$, 400 MHz), • $_{ppm}$: 8.17 (2H, *s*, H-6, H-7), 7.92 (2H, *dd*, *J* = 1.2, 4 Hz, H-5'), 7.52 (2H, *dd*, *J* = 1.2, 5.2 Hz ,H-3'), 7.35-7.21 (6H, *m*, H-4'', H-5'', H-6''), 7.19 (2H, *dd*, *J* = 4, 5.1 Hz, H-4'), 6.90-6.87 (2H, *m*, H-2''), 1.01 (18H, *s*, H-4'''), 0.19 (12H, *s*, H-1'''); ^{13}C-NMR ($CDCl_3$, 100.6 MHz), • $_{ppm}$: 155.7 (C-3''), 151.5 (C-2, C-3), 140.1 (C-9,C-

10), 138.8 (C-2'), 137.1 (C-5,C-8), 131.2 (C-1''), 129.3 (C-5''), 128.7 (C-6,C-7), 127.1 (C-4'), 126.7 (C-3'), 126.5 (C-5'), 123.6 (C-6''), 121.8 (C-4''), 121.1 (C-2''), 25.7 (C-4'''), 18.2 (C-3'''), -4.3 (C-1''').

6.3.6. 5,8-Bis(5-bromothiophen-2-yl)-2,3-bis(3-(*tert*-butyldimethylsilyloxy)phenyl)-quinoxaline (48)

Compound **47** (1.55 g, 2.192 mmol) was dissolved in THF (100 mL) in a round bottomed flask. NBS (0.78 g, 4.38 mmol) was added in one portion and the mixture was stirred under nitrogen, in the dark, overnight. Thin layer chromatography revealed two spots-the monobrominated and the desired product. Another portion of NBS (10 mg, 0.06 mmol) was added and the reaction was allowed to continue for 1h. Thin layer chromatography still showed incomplete conversion and therefore, portions of 15 mg of NBS were added in one hour intervals. When a total amount of 0.83 g NBS (4.63 mmol) had been added, thin layer chromatography indicated full conversion. The reaction mixture was poured on to water and was extracted with dichloromethane. The organic layer was collected and washed with brine and distilled water. The dichloromethane-soluble portion was dried over anhydrous Na_2SO_4 and removal of the solvent gave 1.86 g of crude product. But the NMR spectrum showed the presence of impurities. Then the mixture was recrystallized from methanol and filtered to afford **48** (0.830 g, 43.7%) as an orange solid.

Mp.166-168 ^{o}C ^{1}H-NMR ($CDCl_3$, 400 MHz), $\bullet_{ppm}$: 8.09 (2H, *s*, H-6, H-7), 7.59 (2H, *d*, *J* = 4 Hz, H-4'), 7.28-7.21 (6H, *m*, H-4'', H-5'', H-6''), 7.14 (2H, *d*, *J* = 4 Hz, H-3'), 6.91(2H, *m*, H-2''), 1.03 (18H, *s,* H-4'''), 0.21 (12H, *s*, H-1'''); ^{13}C-NMR ($CDCl_3$, 100.6 MHz), $\bullet_{ppm}$: 155.8 (C-3''), 152.1 (C-2,C-3), 139.6 (C-2', C-9, C-10), 136.5 (C-5,C-8), 130.7 (C-1''), 129.4 (C-4'), 129.2 (C-5''), 125.8 (C-6, C-7), 125.7 (C-3'), 123.6 (C-6''), 121.7 (C-4''), 121.2 (C-2''), 117.1 (C-5'), 25.7 (C-4''') , 18.2 (C-3''') , -4.2 (C-1''').

6.3.7. 3,3'-(5,8-Bis(5-bromothiophen-2-yl)quinoxaline-2,3-diyl)diphenol (49)

Compound **48** (0.6 g, 0.69 mmol) was dissolved in THF (20 mL) and to this was added a 1M solution of tetrabutylammonium fluoride (1.0 mL, 3.469 mmol) drop-wise using syringe. After the addition of the TBAF solution was complete, the orange color of the solution changed to dark red color and stirring continued at room temperature overnight under nitrogen atmosphere. The presence of unreacted starting material was detected by thin layer chromatography using chloroform:methanol (4.8:0.2), and of TBAF (0.1 mL) was added and stirring continued for an additional 5 h. Then water was added and the mixture was extracted with chloroform and small amount of methanol was added to facilitate the dissolution of the mixture. Acidification of the mixture with 2 M HCl promoted the solubility. The organic layer was washed with brine and distilled water, dried over anhydrous Na_2SO_4. Up on removal of the solvent, an orange solid was obtained which was chromatographed on silica gel using chloroform:methanol (4.8 :0.8) solvent system to afford compound **49** (0.266 g, 60.3%) as an orange-red solid.

^{1}H-NMR ($CDCl_3$, 400 MHz), • $_{ppm}$: 8.07 (2H, *s*, H-6,H-7), 7.58 (2H, *d*, *J* = 4.4Hz, H-4'), 7.28-7.19 (8H, *m*, H-4'', H-5'', H-6'', H-1'''), 7.13 (2H, *d*, *J* = 4 HZ, H-3'), 6.96 (2H, *m*, H-2''); ^{13}C-NMR ($CDCl_3$, 100.6 MHz), • $_{ppm}$: 155..8 (C-3''),151.8 (C-2, C-3),139.6 (C-2', C-9, C-10),136.6 (C-5,C-8), 130.6 (C-1''),129.5 (C-4'), 129.2 (C-5''),125.8 (C-6, C-7),125.7 (C-3'),122.8 (C-6''),117.2 (C-4''),117.1 (C-5'),116.5 (C-2'').

6.3.8 5,8-Bis(5-bromothiophen-2-yl)-2,3-bis(3-(2-(2-methoxyethoxy)ethoxy) phenyl) quinoxaline (50)

Compound (**49**) (0.266 g, 0.42 mmol) was dissolved in DMF (15 mL) and to it was added K_2CO_3 (2 g, 0.0145 mol). The mixture was heated at 100 ^{0}C and 1-chloro-2-(2-methoxyethoxy)ethane (0.1232 mg, 0.89 mmol) was added drop-wise from a pressure-equalizing dropping funnel. Heating continued overnight and then the mixture was cooled and filtered. The filtrate was washed with 5% NaOH, extracted with chloroform,

washed with 2M HCl and distilled water, dried over anhydrous Na_2SO_4 and evaporation of the solvent afforded compound **50** (79.68%, 0.280 g) as dark-red solid.

MP.168-170 ^{1}H-NMR ($CDCl_3$, 400 MHz), • $_{ppm}$: 7.75 (2H, *s*, H-6,H-7), 7.53 (2H, *s*, H-6''), 7.32 (2H, *d*, *J* = 4 Hz H-4'), 7.22 (2H, *t*, *J* = 7.8, 7.6 Hz H-5''), 7.04(6H, *m*, H-2'', H-4'', H-3'), 4.24 (4H, *t, J* = 8.8 Hz, 1'''), 3.94 (4H, *t*, *J* = 8.8 Hz, H-2'''), 3.77 (4H, *t*, *J* = 9.2 Hz, H-4'''), 3.62 (4H, *t, J* = 9.2 Hz, H-5'''), 3.43 (6H, *s*, H-7'''); ^{13}C-NMR ($CDCl_3$, 100.6 MHz), • $_{ppm}$: 159.0(C-3''), 151.3 (C-2,C-3), 139.3 (C-9, C-10), 139.1 (C-2'), 136.0 (C-5, C-8), 130.0 (C-1''), 129.1 (C-5''), 128.9 (C-6, C-7), 125.3 (C-4'), 125.2 (C-3'), 123.3 (C-4''), 117.5 (C-6''), 117.1 (C-5'), 72.0 (C-5'''), 70.8 (C-4'''), 69.8 (C-2'''), 67.8 (C-1'''), 59.1 (C-7''').

6.3.9 Synthesis of 9,9-bis(2-(2-methoxyethoxy)ethyl)-9*H*-fluorene

Fluorene (8 g, 48.1 mmol) was dissolved in THF (120 mL) and cooled to -78 ^{o}C. 2.5 M *n*-BuLi (20 mL, 50 mmol) was added and the mixture was stirred for 30 min at the same temperature. 1-Chloro-2-(2-methoxyethoxy)ethane (6.8 g, 49.1 mmol) was then added and stirring continued for 1 h at • 78 ^{o}C followed by stirring at room temperature for 30 min. The cooling bath was placed back and the reaction mixture was cooled to • 78 ^{o}C. 2.5 M *n*-BuLi (24 mL, 60 mmol) was added and the mixture was stirred for 45 min. Then, 1-chloro-2-(2-methoxyethoxy)ethane (7.2 g, 52 mmol) was added. After stirring at • 78 ^{o}C for 30 min, the immersion cooler was turned off and the mixture was allowed to warm to room temperature gradually overnight. The mixture was quenched by adding water and the aqueous phase was extracted with diethyl ether. The combined organic phase was washed with distilled water and dried over anhydrous Na_2SO_4. The solvent was removed on a rotary evaporator and the oily crude product was passed through a column of silica gel using chloroform and chloroform-methanol (4.9:0.1) solvent systems and 9,9-bis(2-(2-methoxyethoxy)ethyl)-9*H*-fluorene was obtained in pure form (5.78 g, 32.4%).

^{1}H-NMR ($CDCl_{3,}$ 400 MHz) • $_{ppm}$: 7.71(2H, *dd*, *J* = 1.2, *J* = 8 Hz), 7.45 (2H, *dd*, *J* = 6.8, *J* = 1.2 Hz), 7.38 (4H, *m*), 3.32(10H, *m*), 3.21 (4H, *t*), 2.77 (4H, *t*), 2.46 (4H, *t*).

6.3.10. Synthesis of 2,7-dibromo-9,9-bis(2-(2-methoxyethoxy)ethyl)-9H-fluorene

9,9-bis(2-(2-methoxyethoxy)ethyl)-9H-fluorene (5.78 g, 15.6 mmol) was dissolved in DMF(80 mL) and bromine (80 mL, 73.75 mmol))dissolved in DMF (5 mL) was added drop-by-drop from a pressure-equalizing dropping funnel over 30 min. Then it was stirred following the progress of reaction by TLC ($CHCl_3$:MeOH (4.9:0.1)). After 115 min, more bromine (1.2 mL) was added and stirring continued overnight. The reaction mixture was quenched with aqueous $Na_2S_2O_3.5H_2O$ solution(10%) and then extracted with diethyl ether. The ether extract was washed with distilled water, dried over anhydrous Na_2SO_4 and the solvent was removed to give an oily material (11.8 g). The crude product was purified by passing through a column packed with silica gel and using $CHCl_3$ and $CHCl_3$:MeOH (4.9:0.1) solvent mixture. 2,7-Dibromo-9,9-bis(2-(2-methoxyethoxy)ethyl)-9*H*-fluorene (8.0 g, 97%) was obtained in a pure form.

^{1}H NMR ($CDCl_{3,}$ 400 MHz) • $_{ppm}$: 7.56 (2H, *d, J* = 1.6 Hz), 7.52 (2H, *s*), 7.49 (2H, *d*, *J* = 1.6 Hz), 3.32 (4H, *t*), 3.3 (6H, *s*), 3.2 (4H, *t*), 2.8 (4H, *t*), 2.39 (4H, *t*).

6.3.11. Synthesis of 2,2'-(9,9-bis(2-(2-methoxyethoxy)ethyl)-9H-fluorene-2,7-diyl)bis(4,4,5,5-tetramethyl-1,3,2-dioxaborolane) (51).

2,7-Dibromo-9,9-bis(2-(2-methoxyethoxy)ethyl)-9*H*-fluorene (8.0 g, 16.01 mmol) was dissolved in dry THF (250 mL) under nitrogen atmosphere and cooled to • 78 ^{o}C. 2.5 M *n*-BuLi (15.8 mL, 40 mmol) was added to the cooled mixture. Then, 2-isopropyl-4,4,5,5-tetramethyl-1,3,2-dioxaborolane (8 g, 32.02 mmol) was added and stirred for some time. Then the immersion cooler was turned off and the mixture was stirred overnight. The reaction mixture was quenched with water and extracted with diethyl ether. The organic phase was dried over anhydrous Na_2SO_4. Up on removal of the solvent, an oily material was obtained which almost solidified on standing. To the crude material, hot petroleum ether was added and the material was dissolved, and when cooled a white material

precipitated. The white solid was collected by suction filtration, dried in a vacuum oven to afford the title compound (2.67 g, 28%).

^{1}H NMR ($CDCl_3$, 400 MHz) • $_{ppm}$: 7.87 (2H, *s)*, 7.83 (2H, *d, J* = 7.2 Hz), 7.73 (2H, *d, J* = 7.6 Hz), 3.32 (4H, *t*), 3.28 (6H, *s*), 3.2 (4H, *t*), 2.69 (4H, *t*), 2.5 (4H, *t*), 1.41 (24H, *s*).

6.4. Polymer Synthesis

6.4.1. Poly[5-(5-(9,9-bis(2-(2-methoxyethoxy)ethyl)-9*H*-fluoren-2-yl)thiophen-2-yl)-2,3-bis(3-(2-(2-methoxyethoxy)ethoxy)phenyl)-8-(thiophen-2-yl)-quinoxaline] (**52**)

Compound **50** (0.100 g, 0.12 mmol), 2-(9,9-bis(2-(2-methoxyethoxy)ethyl)-7-(4,4,5,5-tetramethyl-1,3,2-dioxaborolan-2-yl)-9*H*-fluoren-2-yl)-4,4,5,5-tetramethyl-1,3,2-dioxaborolane (**51**) (0.074 g, 0.12 mmol) and $Pd(PPh_3)_4$ (0.014 g, 0.012 mmol) were placed in a 25 mL round bottomed flask containing toluene (10 mL) under nitrogen. The whole content was heated to reflux for 10 min. To the refluxing mixture tetraethylammonium hydroxide (0.505 mL, 3.56 mmol) was added using a syringe via a septum. The refluxing continued overnight. Bromobenzene (0.1 mL, 9.5 mmol) was added and the mixture was refluxed for 1 h. Phenyl boric acid (0.131 g, 1.2022 mmol) was introduced and refluxing continued for 1 h. The mixture was then added to a flask containing methanol slowly. The solid formed was collected by suction filtration. The solid was dissolved in chloroform and ammonia was added and stirred for one night. The washing was repeated with fresh ammonia for the second time. The chloroform layer was concentrated to a small volume and the polymer was again precipitated by pouring to a flask containing methanol. The solid was collected by suction filtration. It was then purified by Soxhlet extraction first with ether and then with chloroform. The ether-soluble portion was discarded. The chloroform extract was concentrated to a small volume and poured into a flask containing methanol. The polymer was collected by suction filtration and dried in a vacuum oven without heating for one night, which finally gave **52** (0.097 g) as a brown powder.

6.4.2. Poly[5-(5-(7-(5-(2,3-bis(3-(tertbutyldimethysilyloxy)phenyl)-8-(5-(9,9-diocthyl-9H-fluoren-2-yl)thiophen-2-yl)quinoxalin-5-yl)thiophen-2-yl)-9,9-diocthyl-9H-fluoren-2-yl)thiophen-2-yl)-2,3-bis(3-(2-(2-methoxyethoxy)ethoxy) phenyl)-8-(thiophen-2-yl)quinoxaline] (**54**)

Compound **50** (0.09 g, 0.11 mmol), 2-(9,9-dioctyl-7-(4,4,5,5-tetramethyl-1,3,2-dioxaborolan-2-yl)-9H-fluoren-2-yl)-4,4,5,5-tetramethyl-1,3,2-dioxaborolane (**51**) (0.086 g, 0.13 mmol), compound **48** (0.023 g, 0.027 mmol) and $Pd(PPh_3)_4$ (0.015 g, 0.013 mmol) were dissolved in toluene (10 mL) under nitrogen. The whole content was heated to reflux for 10 min. To the refluxing mixture tetraethylammonium hydroxide (0.57 mL, 4.015 mmol) was added using a syringe via a septum. The refluxing continued overnight and the growing polymer chains were end-capped with bromobenzene (0.11 mL, 1.07 mmol) and phenyl boric acid (0.15 g, 1.20 mmol) where each time the mixture was refluxed for one hour. The mixture was then added dropwise to a flask containing methanol. The solid formed was collected by suction filtration. The solid was dissolved in chloroform and ammonia was added and stirred for one night. The washing was repeated with fresh ammonia for the second time. The chloroform layer was concentrated to a small volume and the polymer was again precipitated by pouring to a flask containing methanol. The solid was collected by suction filtration. It was then purified by Soxhlet extraction first with ether and then with chloroform. The ether-soluble portion was discarded. The chloroform extract was concentrated to a small volume and poured to a flask containing methanol. The polymer was collected by suction filtration and dried in vacuum oven without heating for one night, which finally gave **54** (0.111 g) as a brown powder.

6.4.2. Attempted Synthesis of Copolymer 55

Polymer **54** (80 mg) was dissolved in THF(10 mL). To the stirred solution, a 1 M solution of tetrabutylammonium fluoride (0.5 mL) was added. The mixture was stirred at room temperature for five days. Distilled water was added to the solution, extracted with

chloroform and washed with distilled water (4x). The organic layer was concentrated to a small volume and added drop-wise into methanol to precipitate the polymer. The solid was isolated by filtration. But, this attempt did not lead to the desired product as confirmed by the ^{1}H-NMR spectrum.

7. REFERENCES

.

1. Charlese, E.; Carraher, J.R. Roy, W.; Tess and Gary W. Poehlein, *Appl. Polym. Sci.*, **1990**, 21.
2. Brabec, C.J.; Sariciftci, N.S.; Hummelen, J.C. *Adv. Funct , Mater.,* **2001**, *11*, 15.
3. Dimitrakopoulos, C.D.; Malenfant, P.R.L. *Adv. Mater.,* **2002**, *14*, 99.
4. Sonmez, G.; Schwendeman I.; Schottland, P.; Zong, K.; Reynolds, J.R. *Macromolecules,* **2003**, *36*, 639.
5. Roncali, J. *Chem. Rev*., **1997**, *97*, 173.
6. McQuade, D.T.; Pullen, A.E.; Swager, T.M. *Chem. Rev*., **2000**, *100*, 2537
7. Dhanabalan, A.; van Duren, J.K.J.; van Hal, P.A.; van Dongen, J.L.J.; Janssen, R.A.J. *Adv. Funct. Mater*., **2001**, *11*, 255.
8. DuBois, C.J.; Reynolds, J.R. *Adv. Mater*., **2002**, *14*, 1844.
9. Bundgaard, E.; Krebs, F.C. *Sol. Energy Mater. Sol. Cells,* **2007**, *91*, 954.
10. Yamamoto, T.; Zhou, Z.; Kanbara, T.; Shimura, M.; Kizu, K.; Maruyama, T.; Nakamura, Y.; Fukuda, T.; Lee, B.L.; Ooba, N.; Tomaru, S.; Kurihara, T.; Kaino, T.; Kubota, K.; Sasaki, S. *J. Am. Chem. Soc.,* **1996**, *118*, 10389.
11. Tanaka, S.; Yamashita, Y. *Synth. Met.,* **1995**, *69*, 599.
12. Kitamura, C.; Tanaka, S.; Yamashita, Y. *Chem. Mater*., **1996**, *8*, 570.
13. Wiberg, K.B.; Lewis, T.P. *J. Am. Chem. Soc.,* **1970**, *92*, 7154.
14. Argiri, T.; Torsten, W.; Bu¨nnagel, T.F.; Markus, S.; Stelios, A.; Choulis,C.; Brabecd, J.; Ullrich S. *J. Mater. Chem.*, **2007**, *17*, 1353.
15. Heravi et al, M.M.; *Catal. Commun.*, **2007**, *8*, 211.
16. Kulkarni, A.P.; Zhu, Y.; Jenekhe, S.A. *Macromolecules,* **2005**, *38*, 1553
17. Thomas, K.R.J.; Velusamy, M.; Jiann, T.L.; Chuen, C.H.; Tao, Y.T. *Chem. Mater.,* **2005**, *17*, 1860.
18. Starke, I.; Sarodnick, G.; Ovcharenko, V.V.; Pihlaja, K.; Kleinpeter, E. *Tetrahedron,* **2004**, *60*, 6063.
19. Zhao, Z.J.; Wisnoski, D.D.; Wolkenberg, S.E.; Leister, W.H.; Wang, Y.; Lindsley, C.W. *Tetrahedron Lett.,* **2004**, *45*, 4873.

20. Brown, D.J.; Quinoxalines: Supplement II, in: E.C. Taylor, P. Wipf (Eds.), *The Chemistry of Heterocyclic Compounds*, John Wiley& Sons, New Jersey, **2004.**
21. Kanbara T., Myazaki Y., Yamamoto T.*, J. Polym. Sci. Part A: Polym. Chem.,* **1995**, *33*, 999.
22. Huo, L.; Tan, Z.; Wang, X.; Zhou, Y.; Han, M.; Li, Y. *J. Polym. Sci. Part A: Polym. Chem*., **2008**, *46*, 4038.
23. Scherf, U.; List, E.J.W. *Adv. Mater*. **2002**, *14*, 477.
24. Suzuki, A. *J. Organomet. Chem.,* **1999**, *576*, 147..
25. Jiao, H.; von, R.; Schleyer, P.; Mo, Y.; McAllister, M.A.; Tidwell, T.T. *J. Am. Chem. Soc.,* **1997**, *119*, 7075.
26. Qibing, P.; Yang, Y. *J. Am. Chem. Soc*., **1996**, *118*, 7416.
27. Chuanjun, X.; Dany, R,; Mario, L. *Macromolecules,* **2001**, *34*,5854.
28. Fukuda, M.; Sawada, K.; Yoshino, K. *Jpn*. *J. Appl. Phys*., **1989**, *28*, 1433.
29. Yamamoto, T. *Macromol. Rapid. Commun.,* **2002**, *23*, 583.
30. Bernius, M.T.; Inbasekaran, M.; O'Brien, J.; Wu, W. *Adv. Mater.,* **2000**, *12*, 1737
31. Hou, Q.; Xu, Y.; Yang, W.; Yuan, M.; Peng, J.; Cao, Y. *J. Mater. Chem*., **2002,** *12*, 2887.
32. Perzon, E.; Wang, X.; Zhang, F.; Mammo, W.; Delgado, J.L.; de la Cruz, P.; Inganäs, O.; Langa, F.; Andersson, M.R. *Synth. Met*., **2005,** *154*, 53.
33. Wang, X.; Perzon, E.; Mammo, W.; Oswald, F.; Admassie, S.; Persson, N.-K.; Langa, F.; Andersson, M.R.; Inganäs, O. *Thin Solid Films*, **2006**, *511*, 576.
34. Zhang, F.; Perzon, E.; Wang, X.; Mammo, W.; Andersson, M.R.; Inganäs, O. *Adv. Funct. Mater*. **2005**, *15*, 745.
35. Gadisa, A.; Mammo, W.; Andersson, L. M.; Admassie, S.; Zhang, F.; Andersson, M. R.; Inganäs, O. *Adv. Funct. Mater.,* **2007**, *17*, 3836.
36. Gedefaw, D.; Zhou, Y.; Stefan, H.; Lindgren, L. Andersson, L. M.; Zhang, F.; Mammo, W.; Inganas, O.; Andersson, M. R. *J. Mater. Chem*., **2009**, *19*, 5359.
37. Neher, D. *Macromol. Rapid Commun*., **2001**, *22*, 1365.
38. Ohmori, Y.; Uchida, M.; Muro, K.; Yushino, K.; *Jpn*. *J. Appl. Phys*., **1991**, *30*, 1941.
39. Wen, C. W.; Chen, L. L.; Wen, C.C., *Polymer*, **2006**, *47*, 527.

40. Peng, Q.; Kang, E. T.; Neoh, K. G.; Xiao, D.; Zou, D. *J. Mater. Chem.,* **2006**, *16*, 376.
41. Lee, J.; Cho, N. S.; Lee, J.; Lee, S. K.; Shim, H. K. *Synth. Met.,* **2005**, *155*, 73.
42. Lee, S. K.; Ahn, T.; Cho, N. S.; Lee, J. I.; Jung, Y. K.; Lee, J.; Shim, H. K. *J. Polym. Sci. Part A: Polym. Chem.,* **2007**, *45*, 1199.
43. Bundgaard, E.; Krebs, F. C. *Sol. Energy Mater. Sol. Cells*., **2007**, *91*, 954.
44. Arias, A. C.; MacKenzie, J. D.; Stevenson, R.; Halls, J. J. M.; Inbasekaran, M.; Woo, E. P.; Richards, D.; Friend, R. H. *Macromolecules*, **2001**, *34*, 6005.
45. Yadessa, M. , *MSc Project Paper*, Department of Chemistry, Addis Ababa University, Et*hiopia, **2007***.
46. *Suz*uki, A.; Miyaura, N. *Chem. Rev.,* **1995**, *95*, 2457.
47. Seung, H.O.; Seok, I. N.; Yoon, C.N.; Doojin, V.; Seok, S.K.; Dong,Y.K. Organic *Electronics* , **2007**, *8*, 773.
48. Pei, Q.; Yang, Y.; Yu, G.; Zhang, C.; Heeger, A.J. *J. Am. Chem. Soc*., **1996**, *118*, 3922.
49. Marsella, M.J.; Swager, T.M.; *J. Am. Chem. Soc*., **1993**, *115*, 12214.
50. Jespersen, K.G.; Beenken, W.J. D.; Zaushitsyn, Y.; Yartsev, A.; Andersson, M.R. Pullerits, T.; Sundström, V. *J. Chem. Phys.,* **2004**, *121*, 12613.
51. Chen, Z.K.; Huang, W.; Wang, L.H.; Kang, E.T.; Chen, B.J.; Lee, C.S.; Lee, S.T. *Macromolecules,* **2000**, *33*, 9015.
52. Shengqiang, X.; Huaxing, Z.; Wei, Y. *Macromolecules,* **2008,** *41*, 5688.

8. APPENDICES

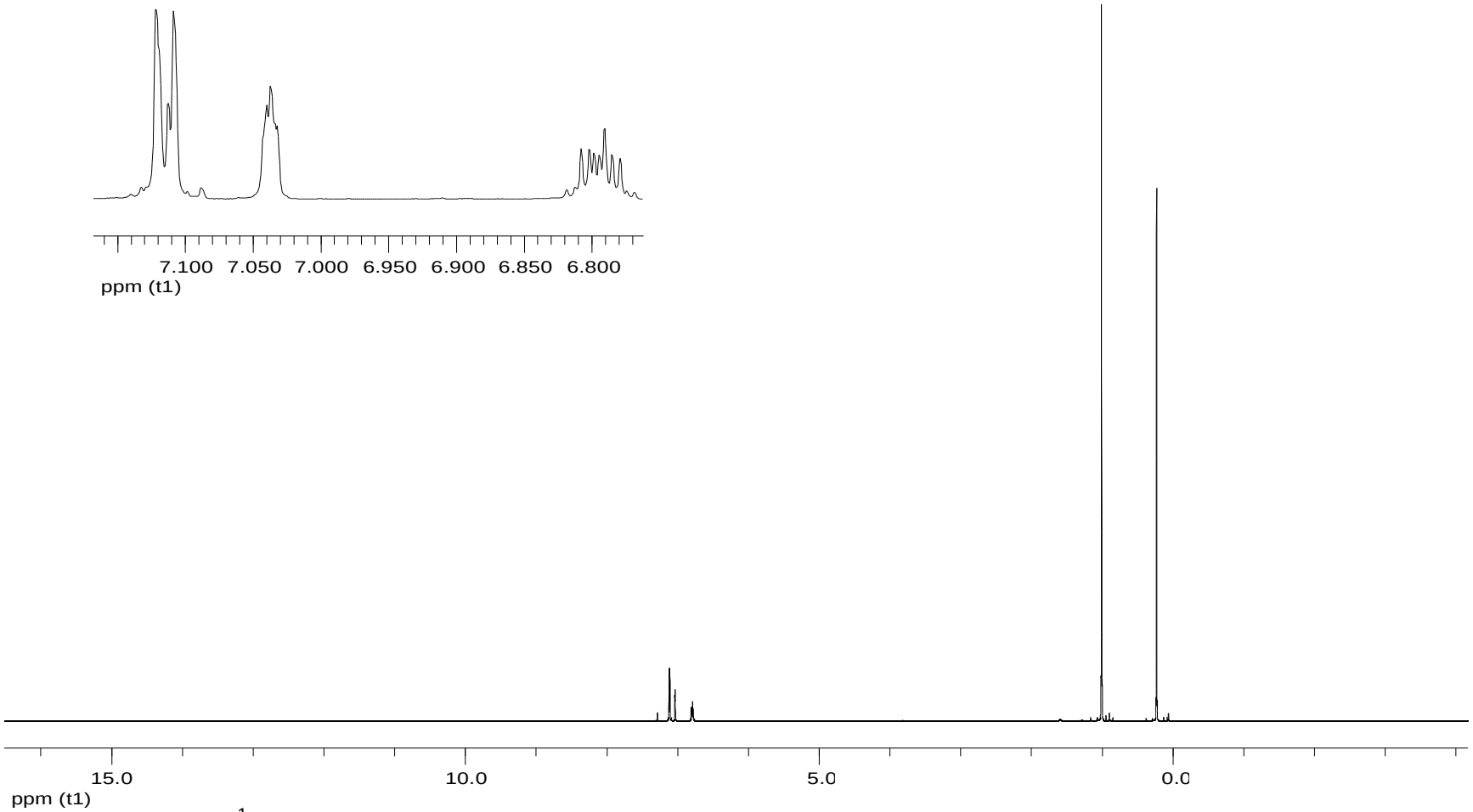

Appendix 1. ^{1}H-NMR ($CDCl_3$, 400 MHz (δ ppm)) spectrum of (3-bromophenoxy)(*tert*-butyl)dimethylsilane (**40**).

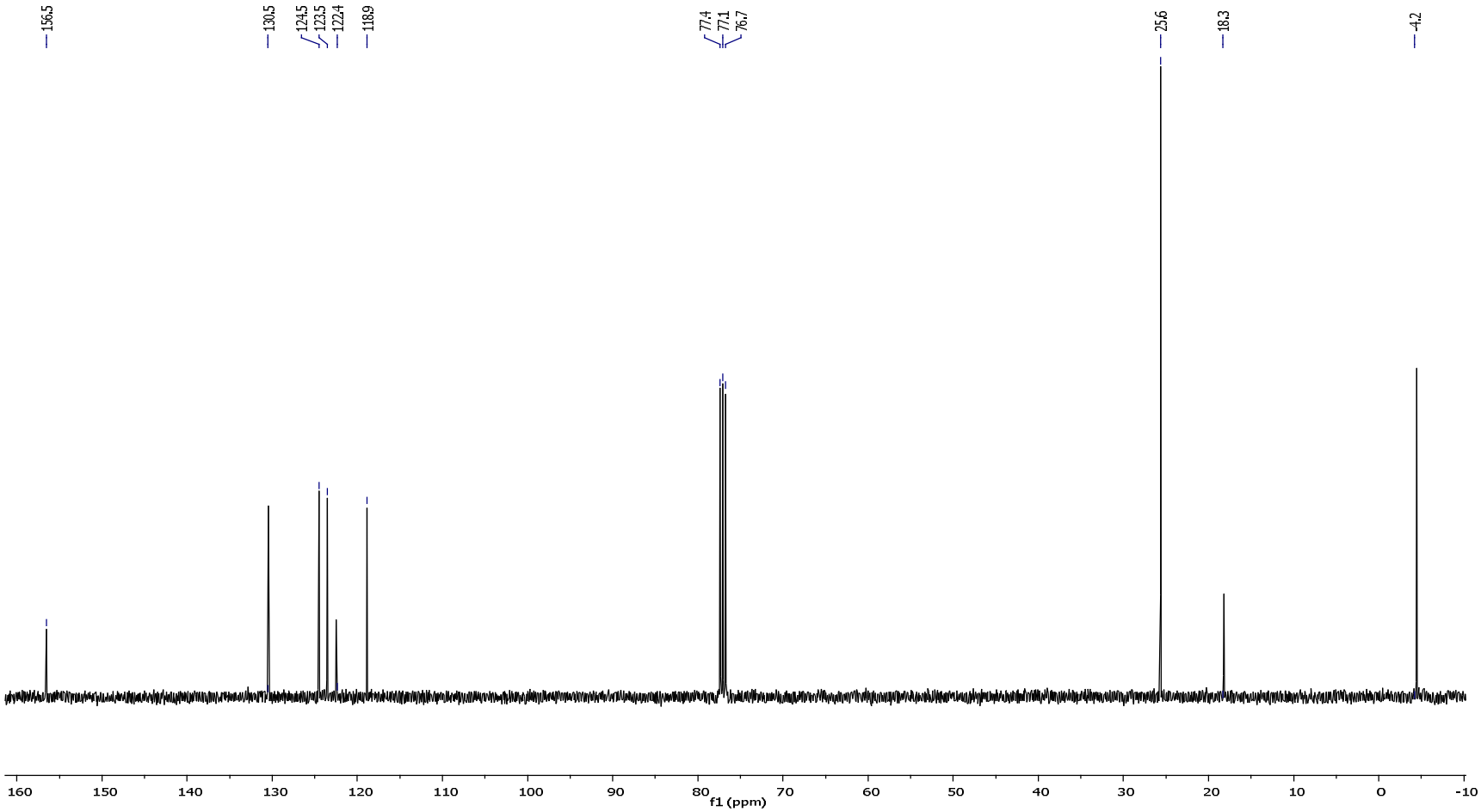

Appendix 2. ^{13}C-NMR ($CDCl_3$, 100.6 MHz (• ppm)) of (3-bromophenoxy)(*tert*-butyl)dimethylsilane (**40**).

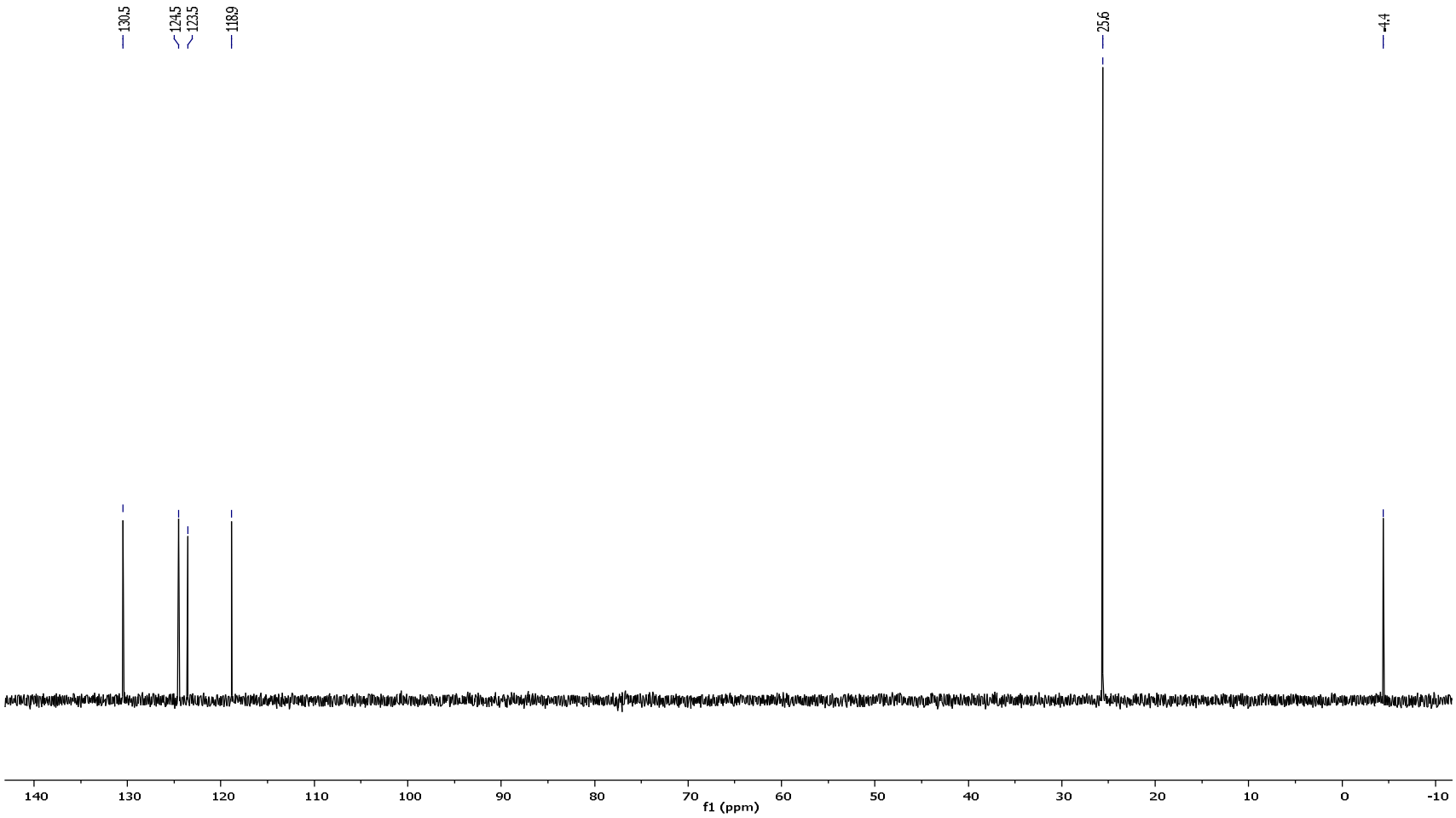

Appendix 3. DEPT-135 spectrum of (3-bromophenoxy)(*tert*-butyl)dimethylsilane (**40**).

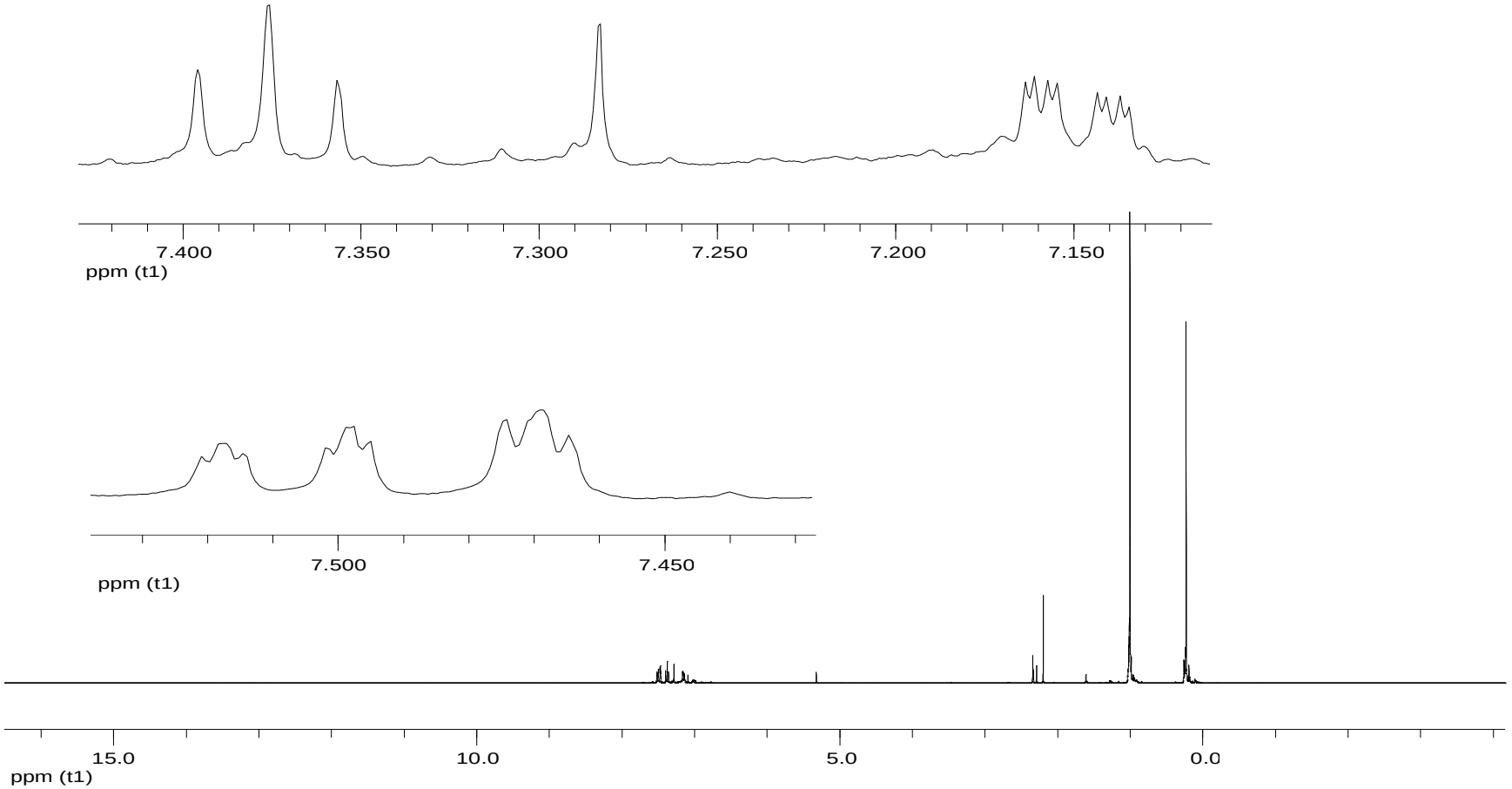

Appendix 1. ^{1}H-NMR ($CDCl_3$, 400 MHz (δ ppm)) spectrum of 1,2-bis(3-(*tert*-butyldimethylsilyloxy)phenyl)ethane-1,2-dione (**41**).

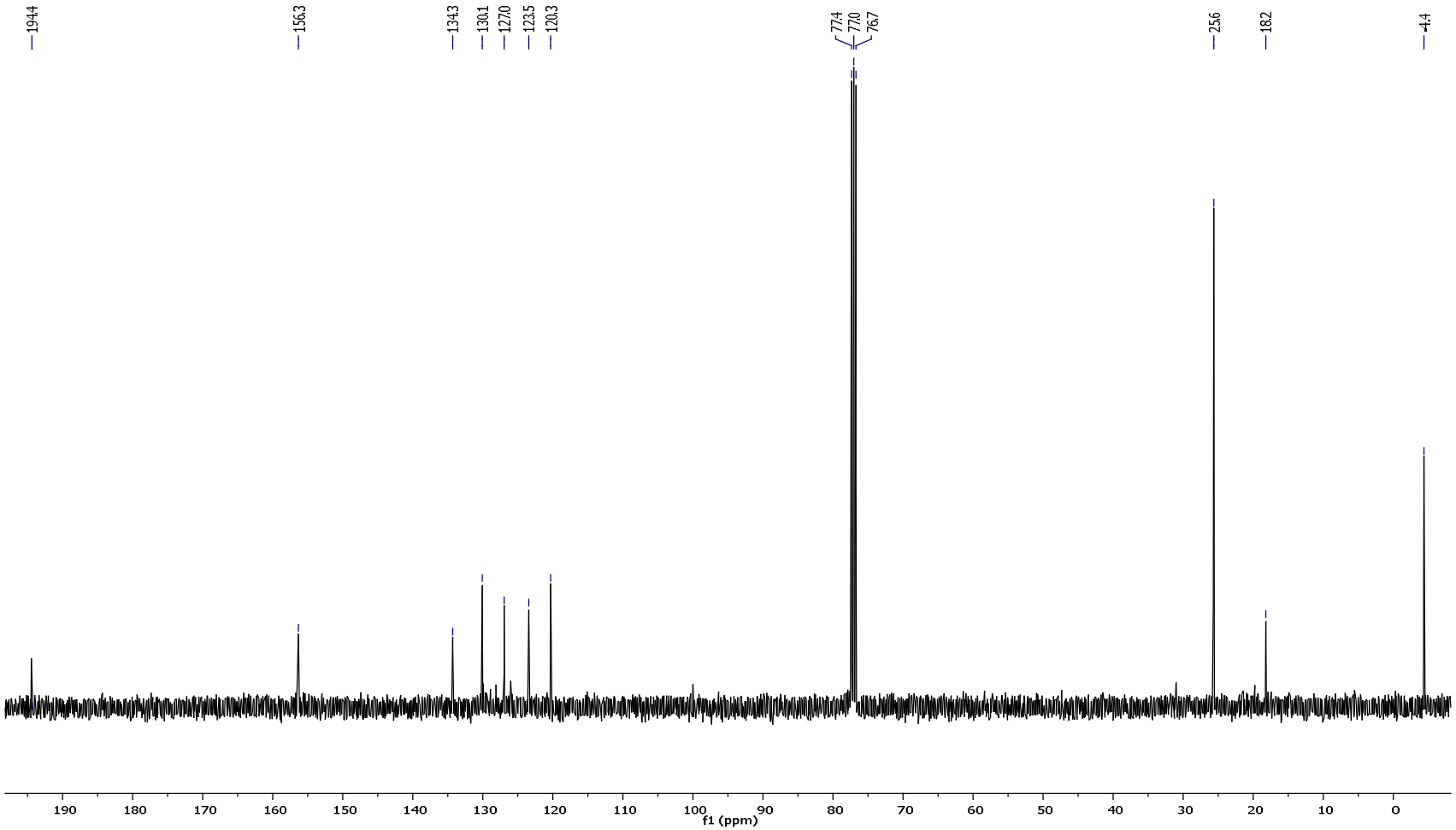

Appendix 5. ^{13}C-NMR ($CDCl_3$, 100.6 MHz (• ppm)) of 1,2-bis(3-(*tert*-butyldimethylsilyloxy)phenyl)ethane-1,2-dione (**41**).

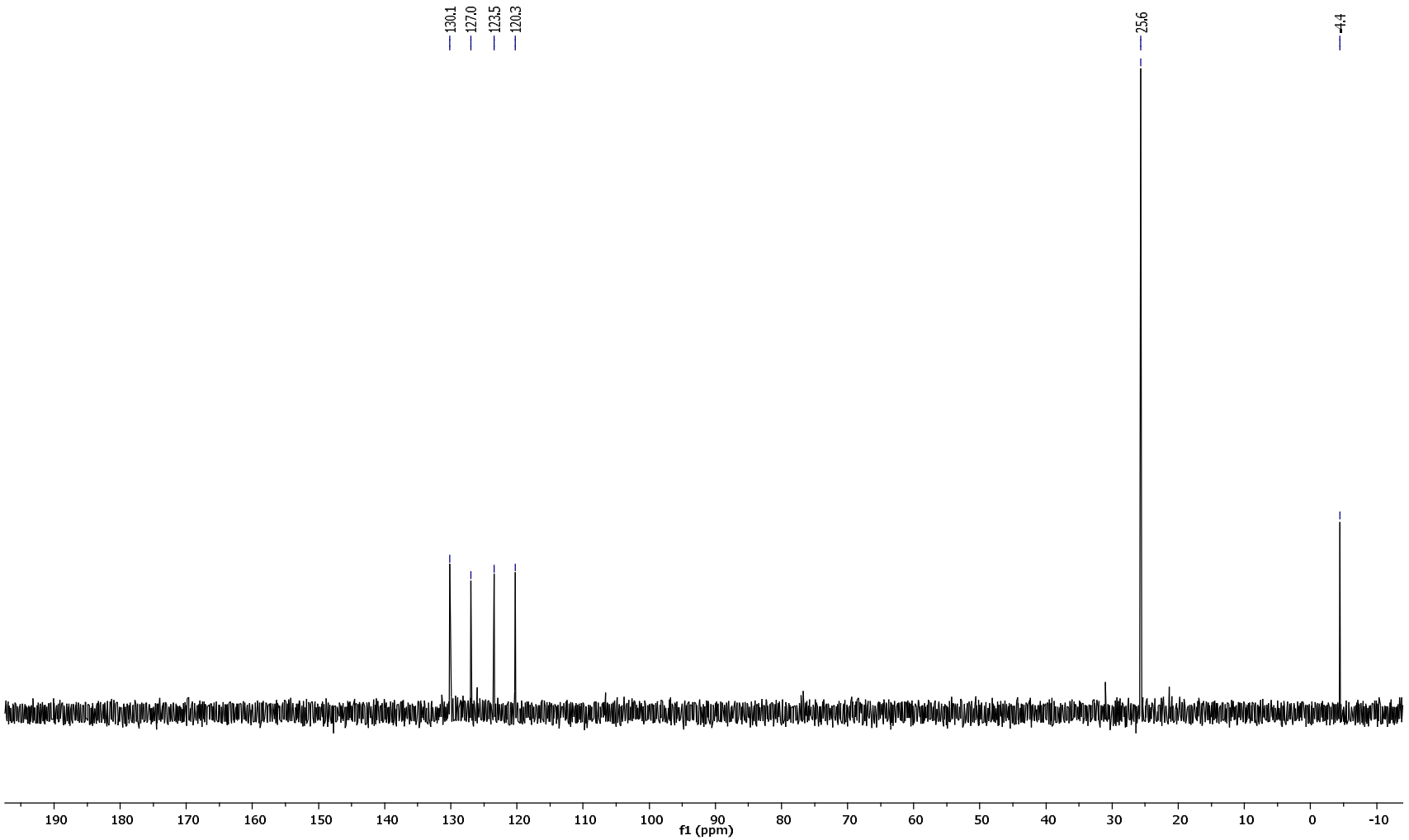

Appendix 6. DEPT-135 spectrum of 1,2-bis(3-(*tert*-butyldimethylsilyloxy)phenyl)ethane-1,2-dione (**41**).

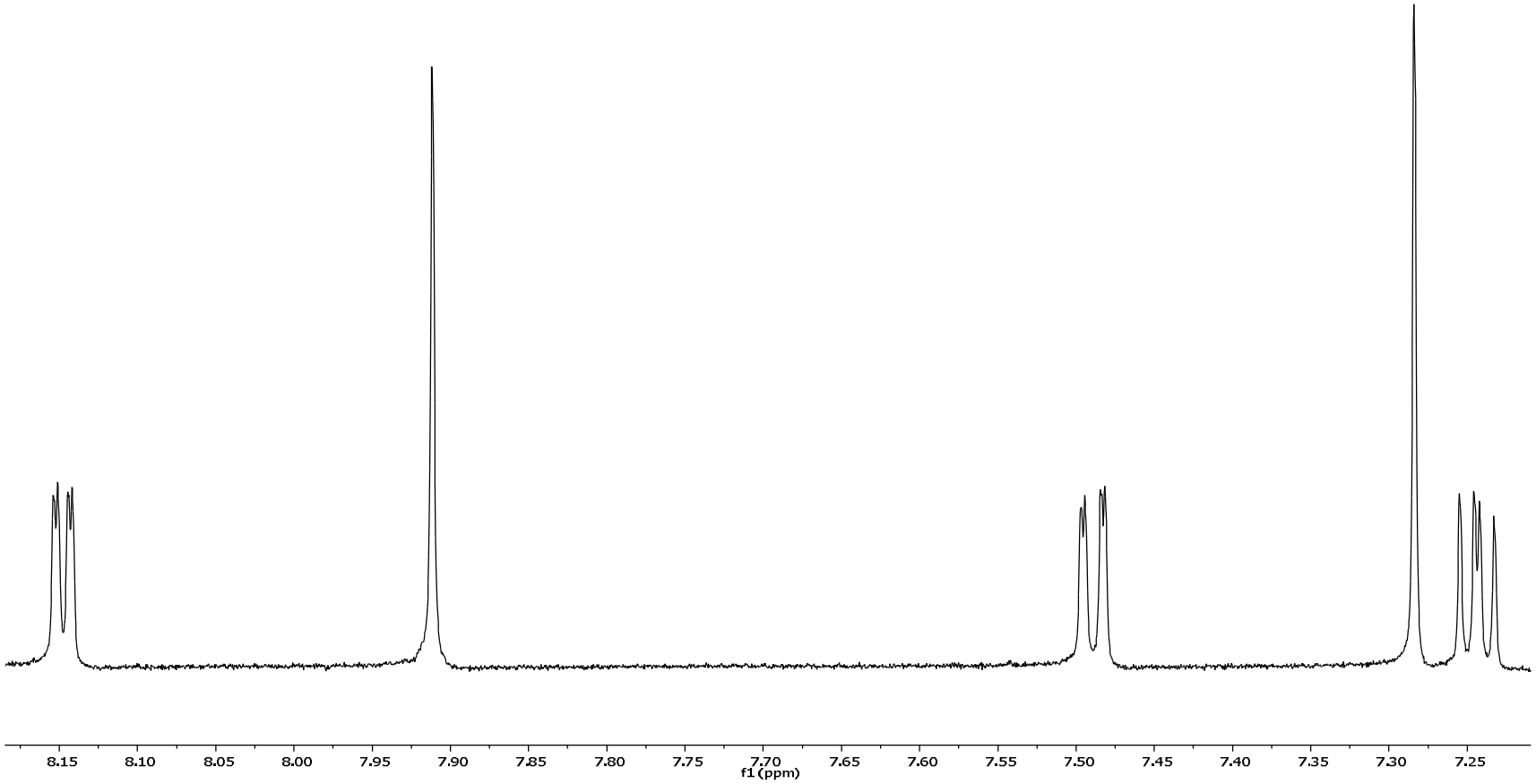

Appendix 7. ^{1}H-NMR ($CDCl_3$, 400 MHz (δ ppm)) spectrum of 4,7-di(thiophen-2-yl)benzo[*c*][1,2,5]thiadiazole (**45**).

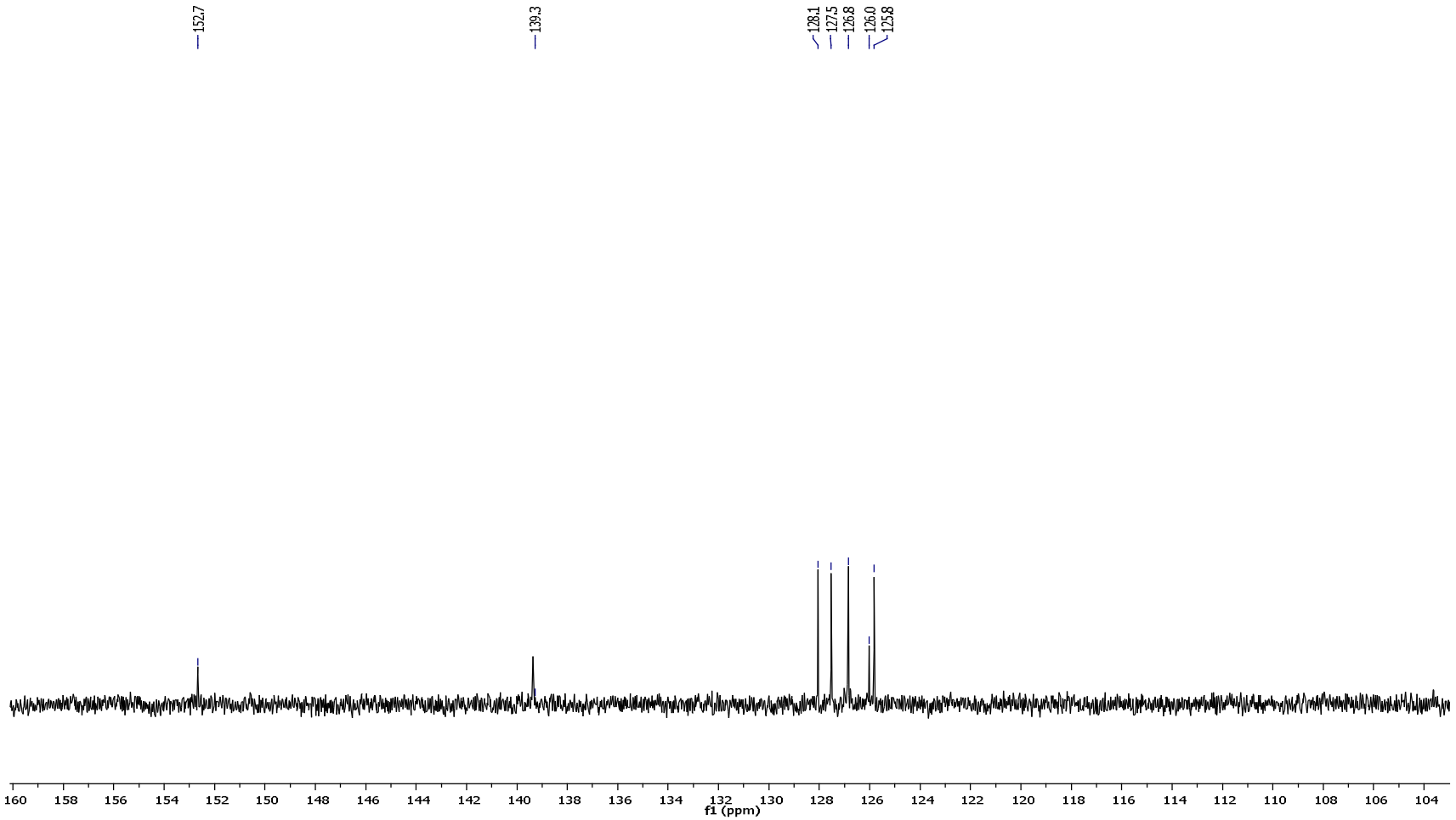

Appendix 8. ^{13}C-NMR ($CDCl_3$, 100.6 MHz (• ppm)) of 4,7-di(thiophen-2-yl)benzo[*c*][1,2,5]thiadiazole (**45**).

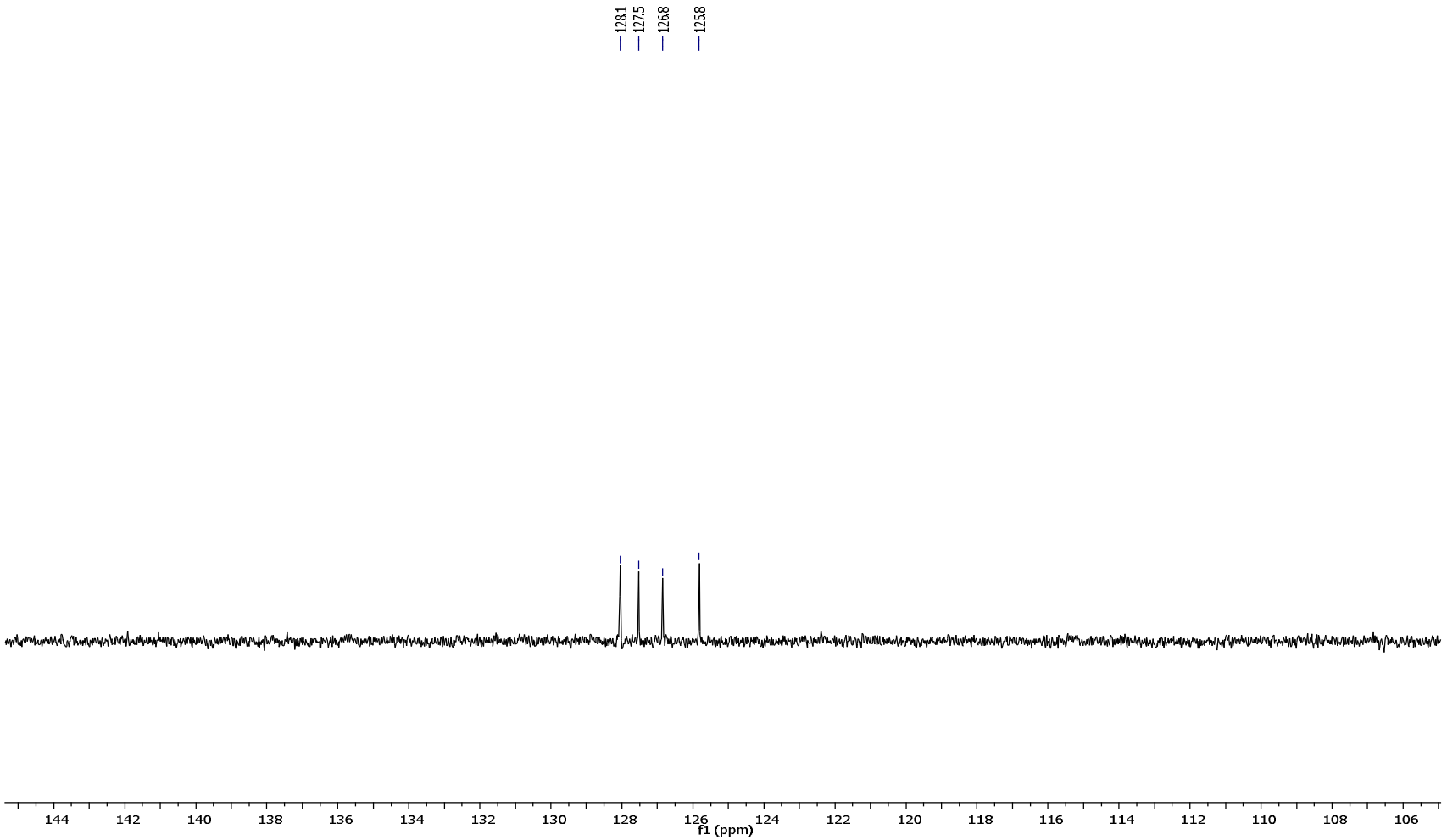

Appendix 9. DEPT-135 spectrum of 4,7-di(thiophen-2-yl)benzo[*c*][1,2,5]thiadiazole (**45**).

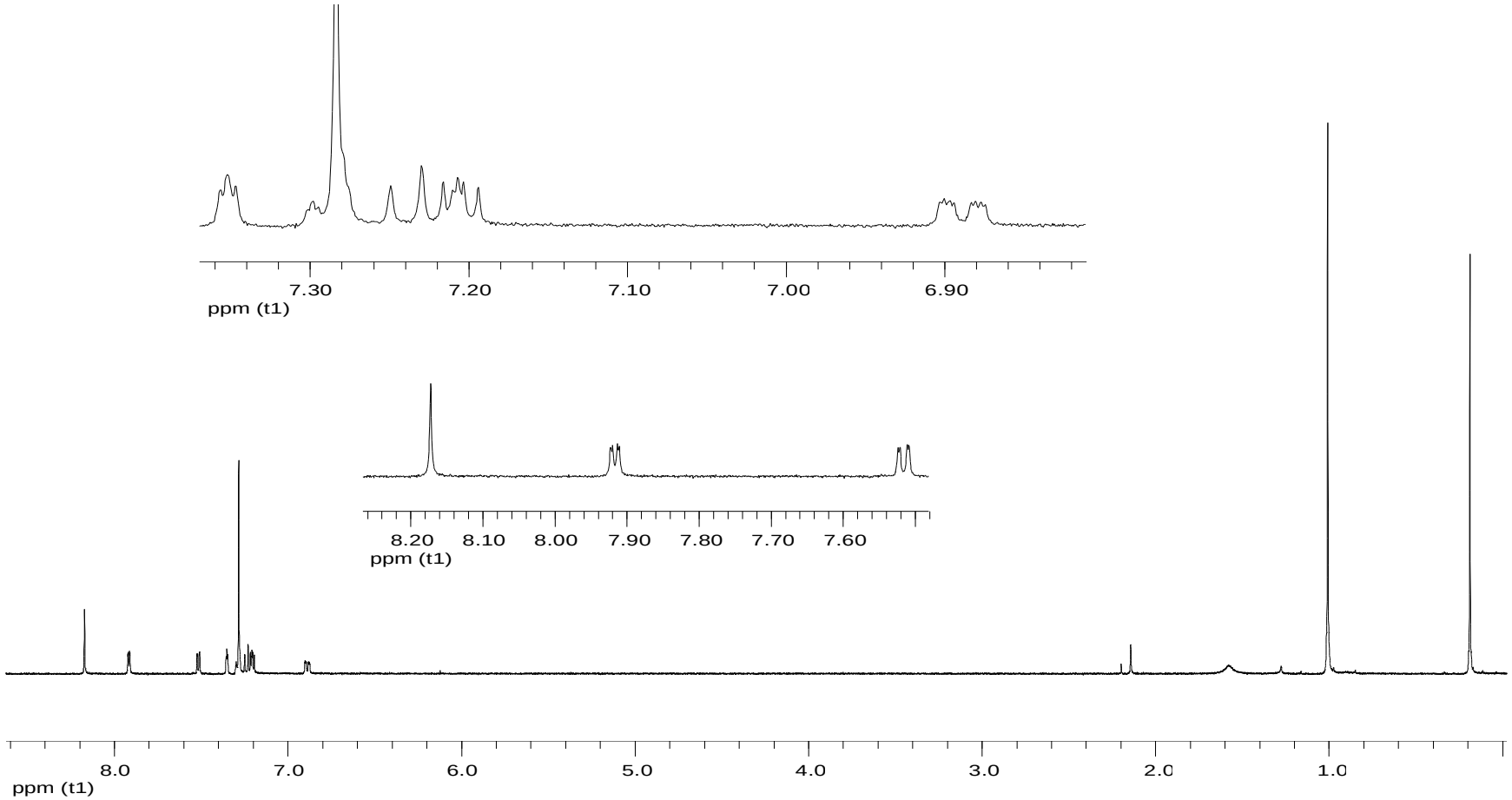

Appendix 10. ^{1}H-NMR ($CDCl_3$, 400 MHz (δ ppm)) spectrum of 2,3-bis(3-(*tert*-butyldimethylsilyloxy)phenyl)-5,8-di(thiophen-2-yl)quinoxaline (**47**).

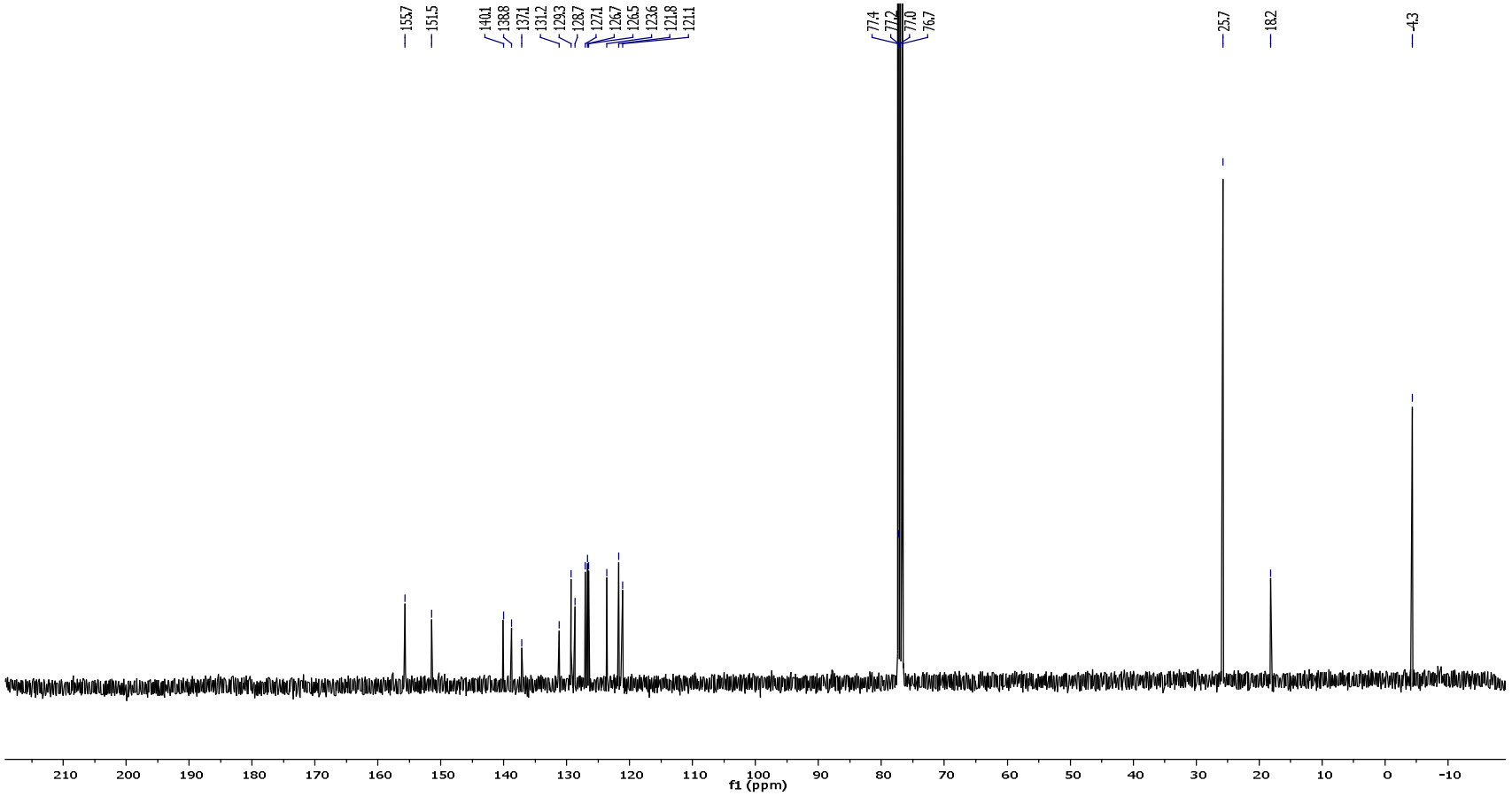

Appendix 11. ^{13}C-NMR ($CDCl_3$, 100.6 MHz (• ppm)) of 2,3-bis(3-(*tert*-butyldimethylsilyloxy)phenyl)-5,8-di(thiophen-2-yl)quinoxaline (**47**).

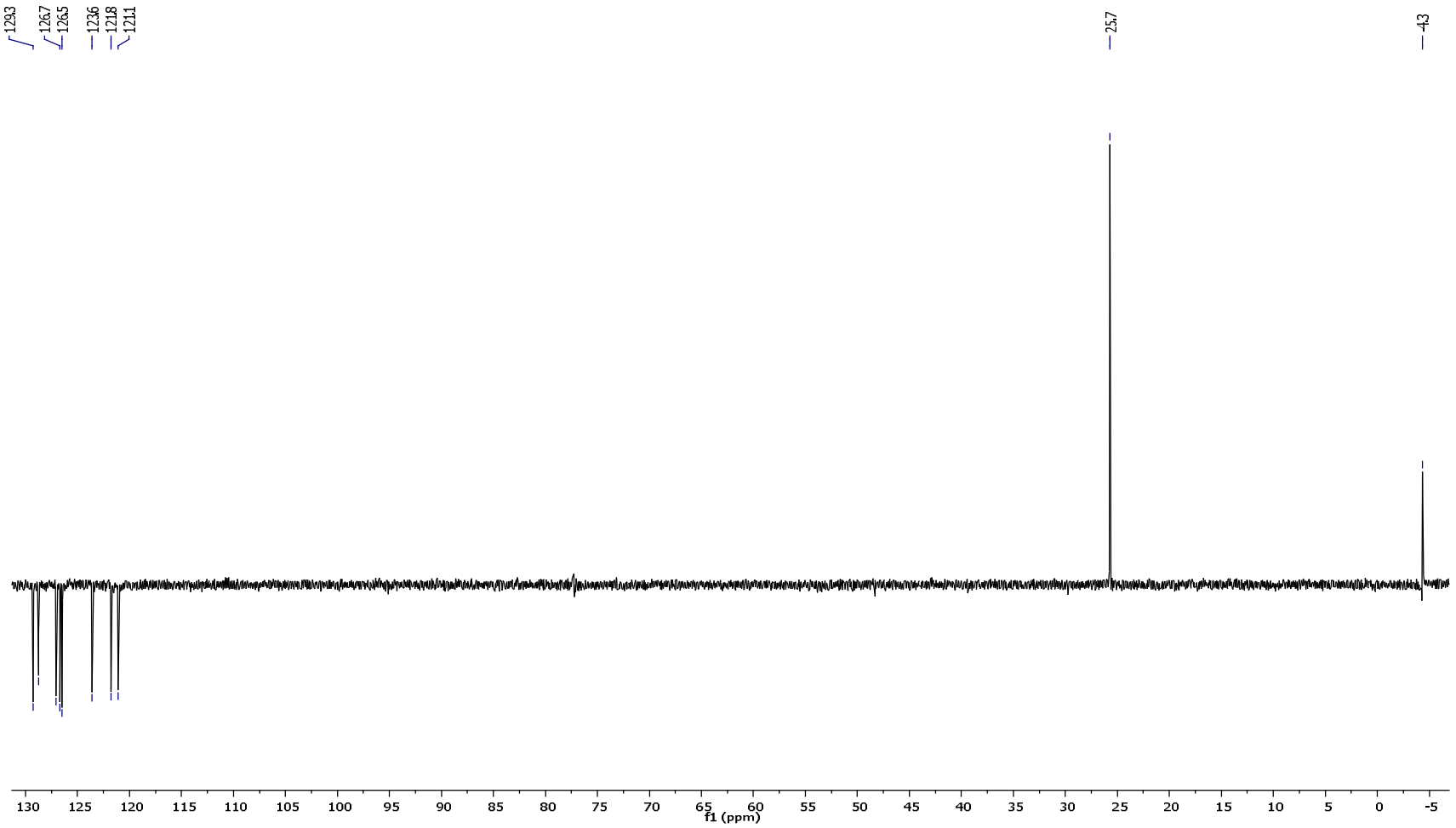

Appendix 12. DEPT-135 spectrum of 2,3-bis(3-(*tert*-butyldimethylsilyloxy)phenyl]-5,8-di(thiophen-2-yl)quinoxaline (**47**).

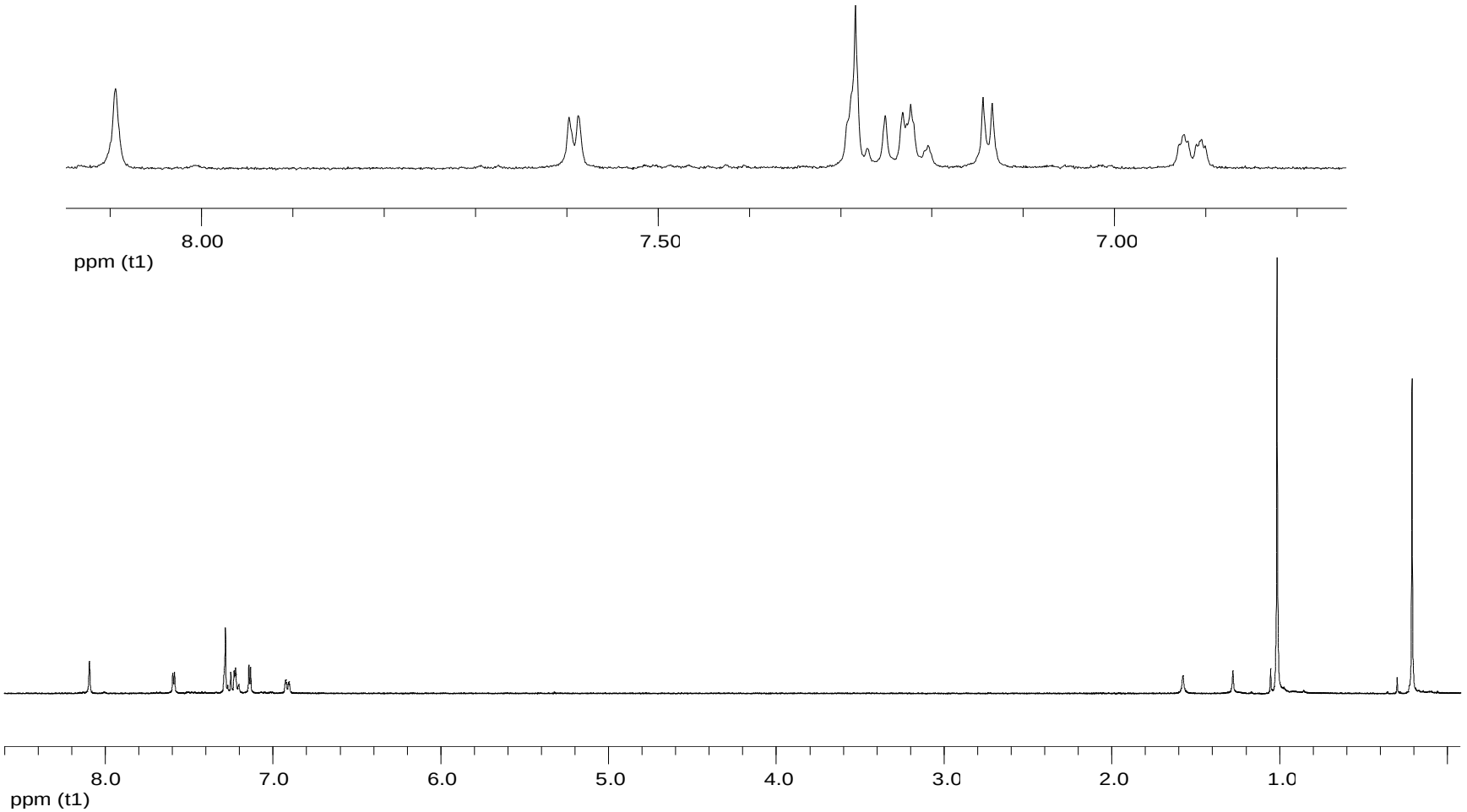

Appendix 13. ^{1}H-NMR ($CDCl_3$, 400 MHz (δ ppm)) spectrum of 5,8-bis(5-bromothiophen-2-yl)-2,3-bis(3-(*tert*-butyl-dimethylsilyloxy)phenyl)quinoxaline (**48**).

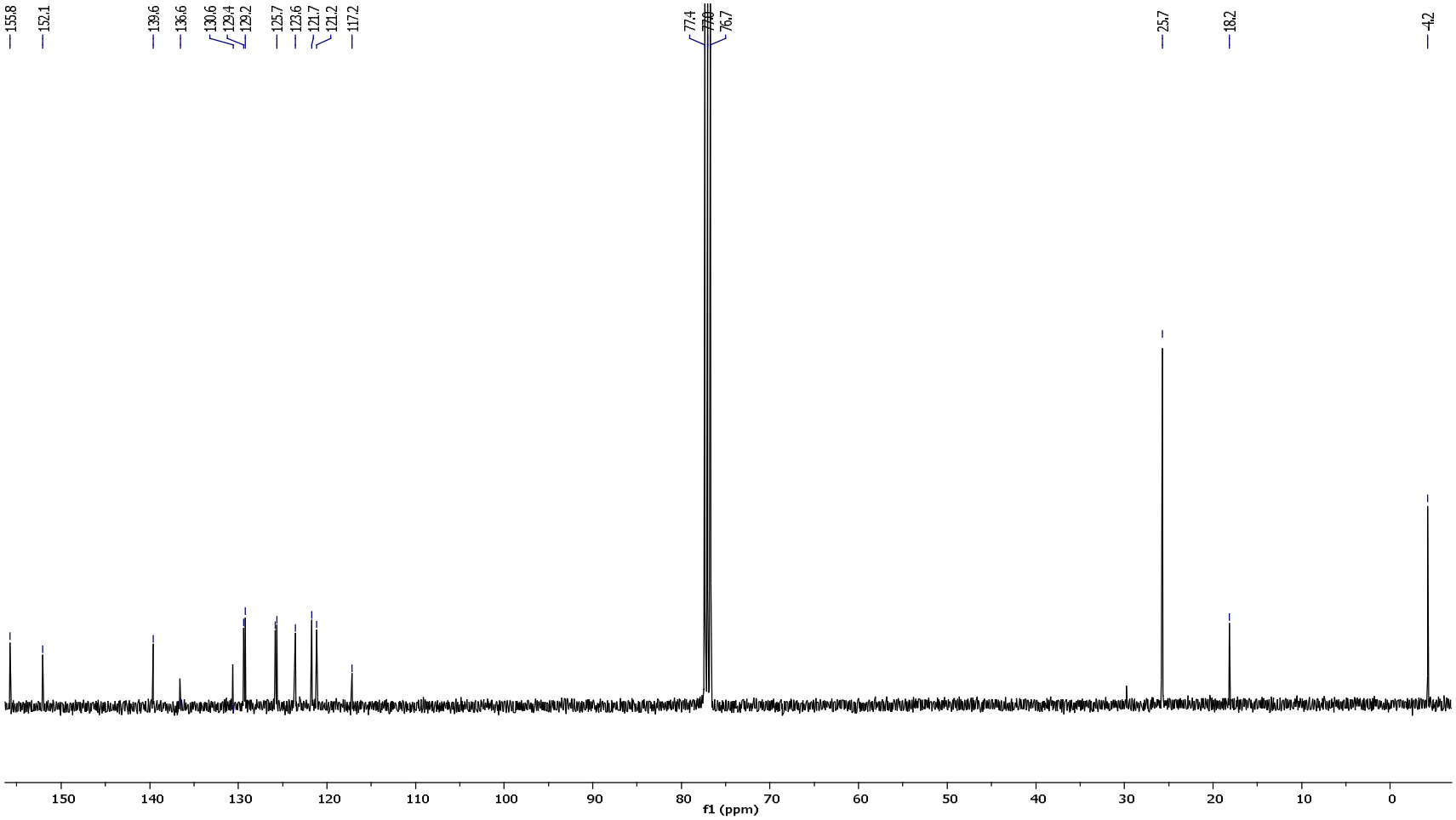

Appendix. 14. ^{13}C-NMR ($CDCl_3$, 100.6 MHz (• ppm)) of 5,8-bis(5-bromothiophen-2-yl)-2,3-bis(3-(*tert*-butyldimethyl-silyloxy)phenyl)quinoxaline (**48**).

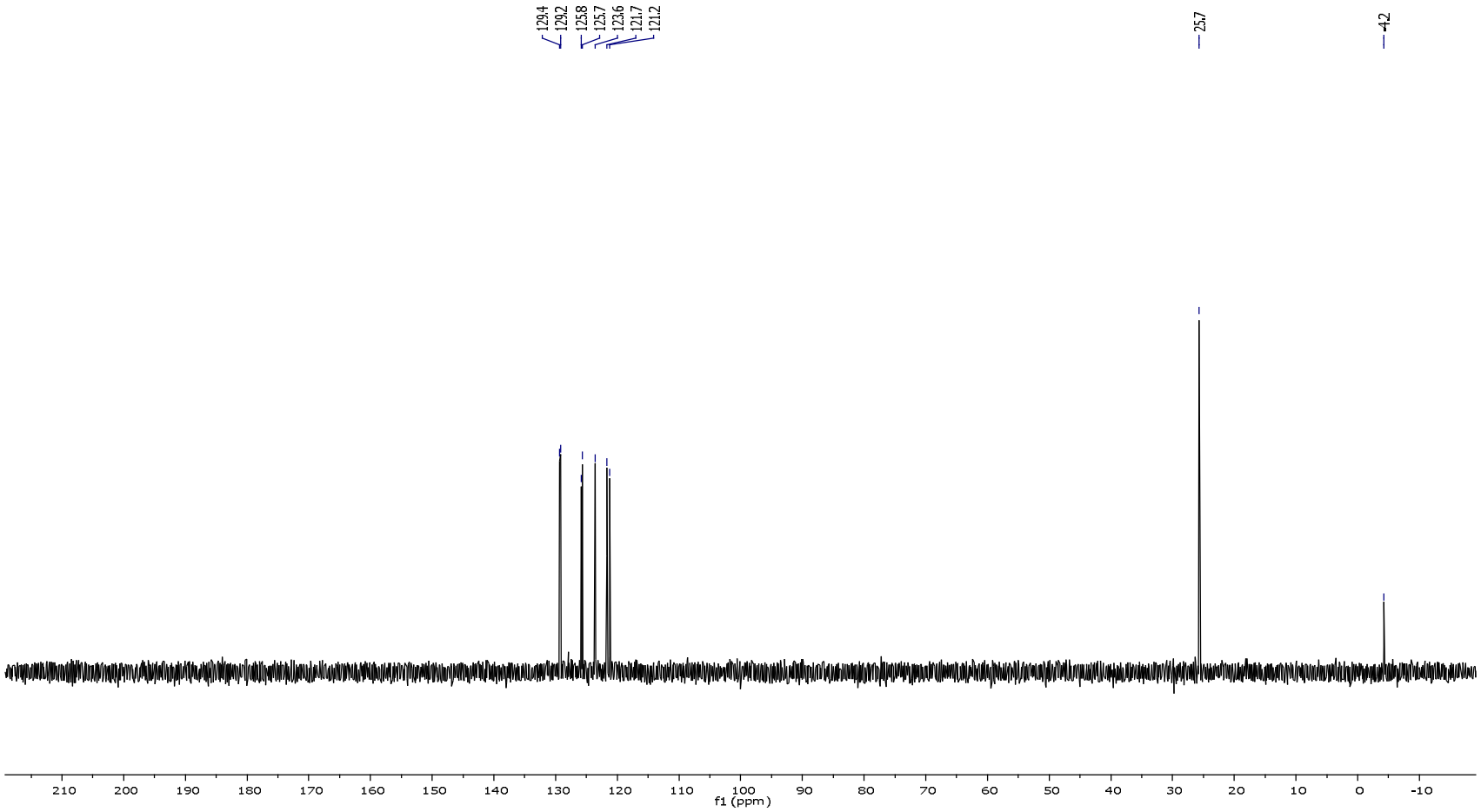

Appendix.15. DEPT-135 spectrum of 5,8-bis(5-bromothiophen-2-yl)-2-3-bis(3-(*tert*-butyldimethysilyloxy)phenyl)-quinoxaline (**48**).

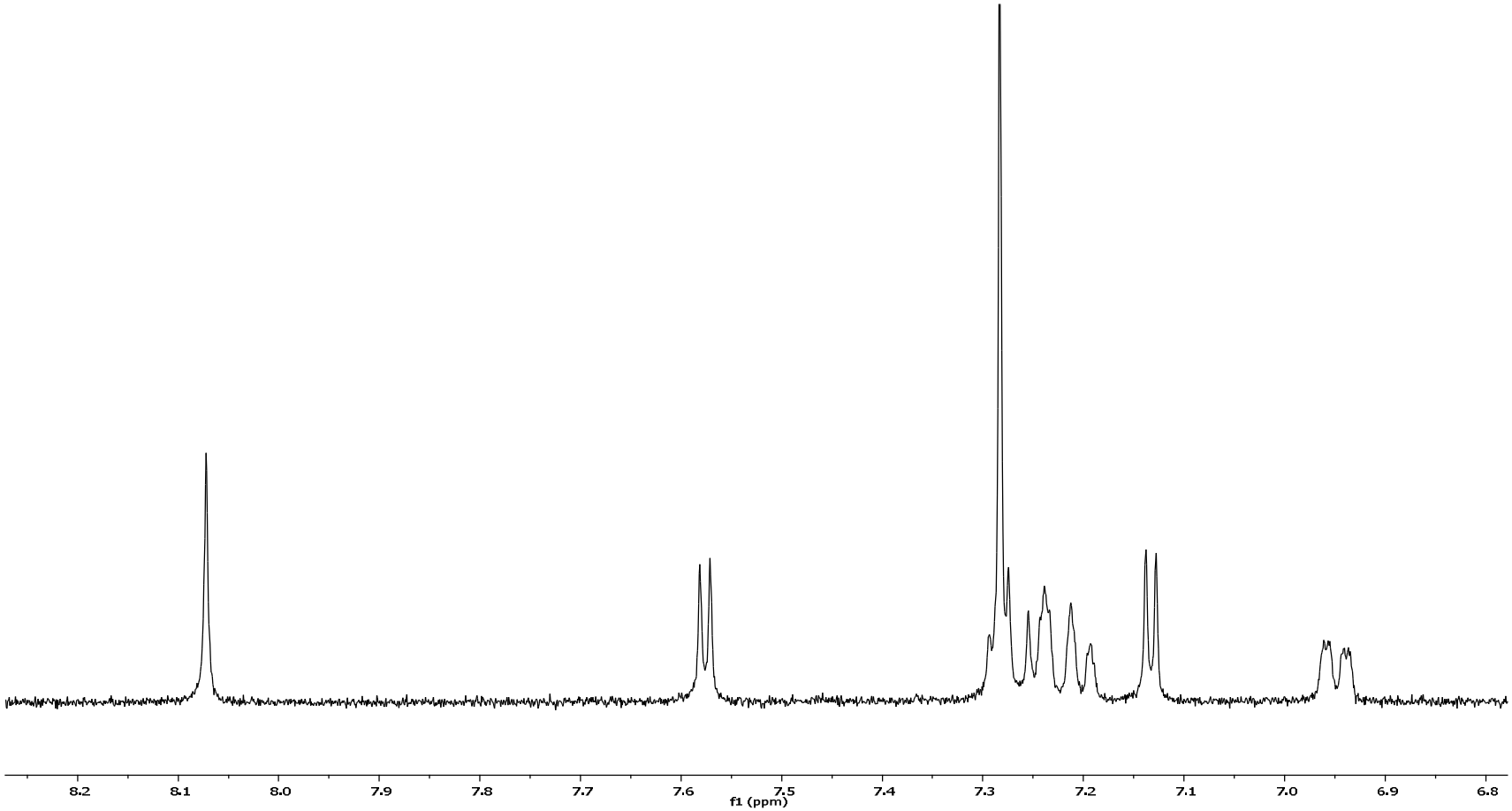

Appendix 16. ^{1}H-NMR ($CDCl_3$, 400 MHz (δ ppm)) spectrum of 3,3'-(5,8-bis(5-bromothiophen-2-yl)quinoxaline-2,3-diyl)diphenol (**49**).

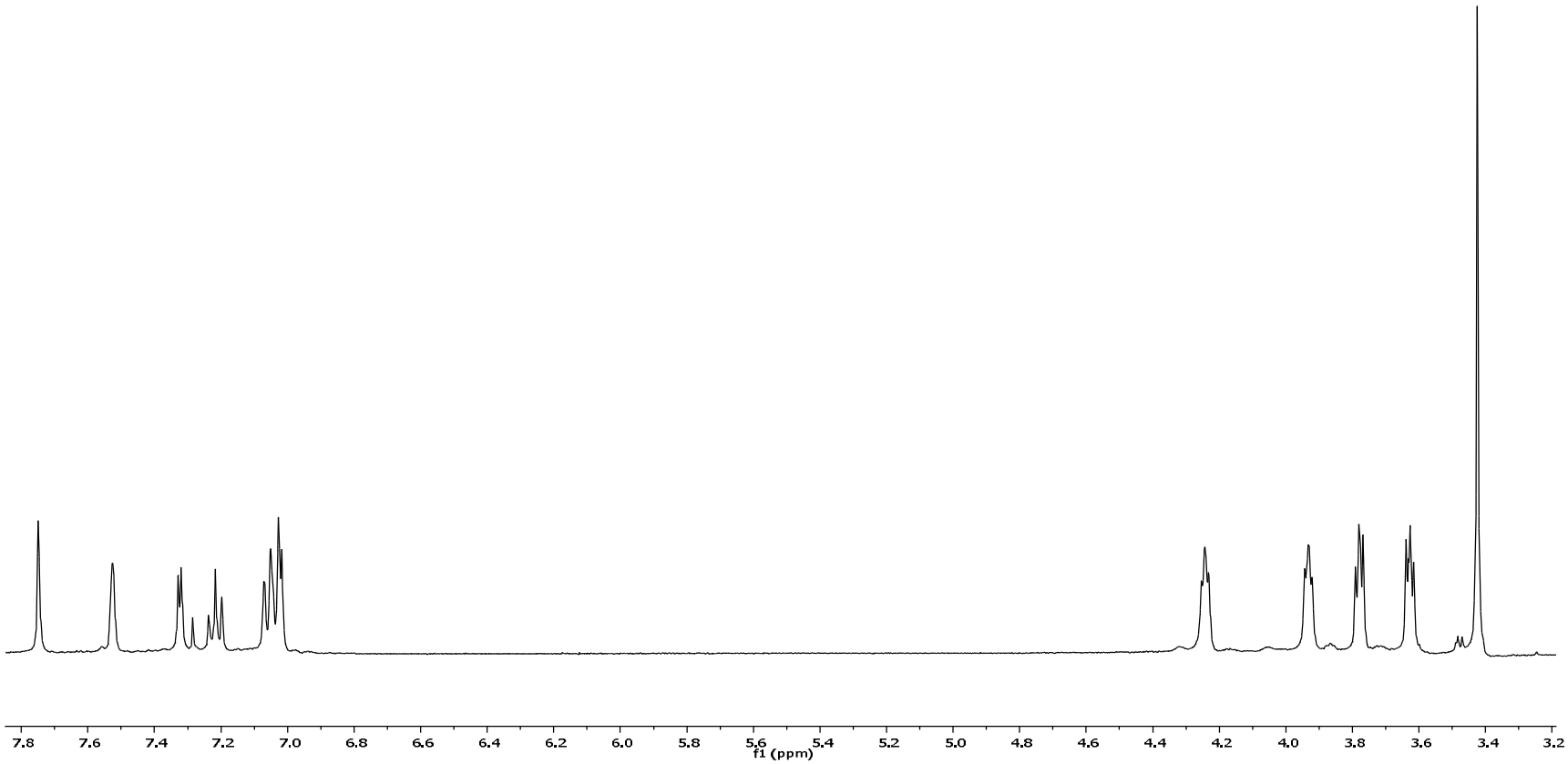

Appendix 17. ^{1}H-NMR ($CDCl_3$, 400 MHz (δ ppm)) spectrum of 5,8-bis(5-bromothiophen-2-yl)-2,3-bis(3-(2-(2-methoxyethoxy)ethoxy)phenyl)quinoxaline (**50**).

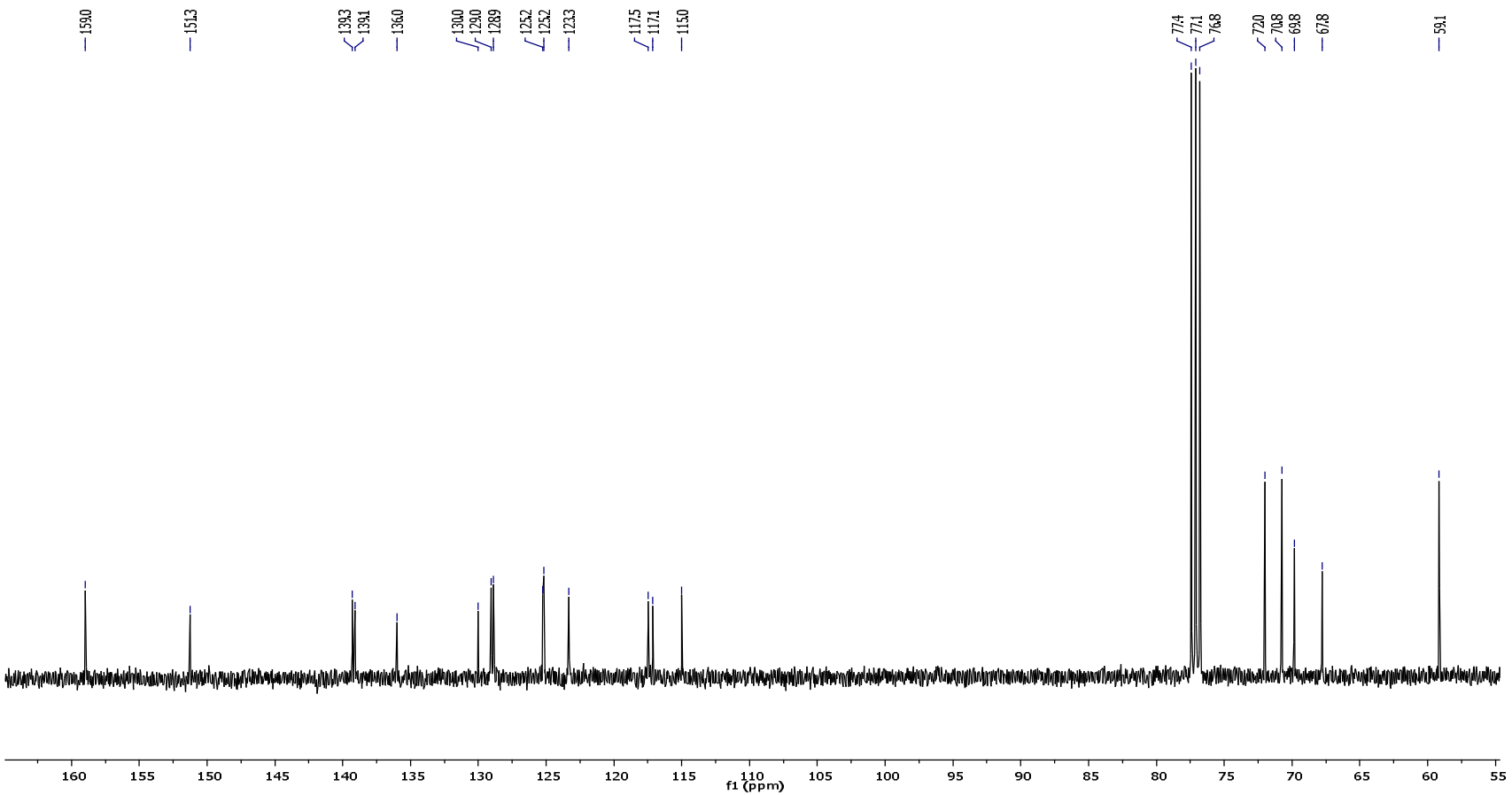

Appendix.18. ^{13}C-NMR ($CDCl_3$, 100.6 MHz (• ppm)) of 5,8-bis(5-bromothiophen-2-yl)-2,3-bis(3-(2-(2-methoxyethoxy)-ethoxy)phenyl)quinoxaline (**50**).

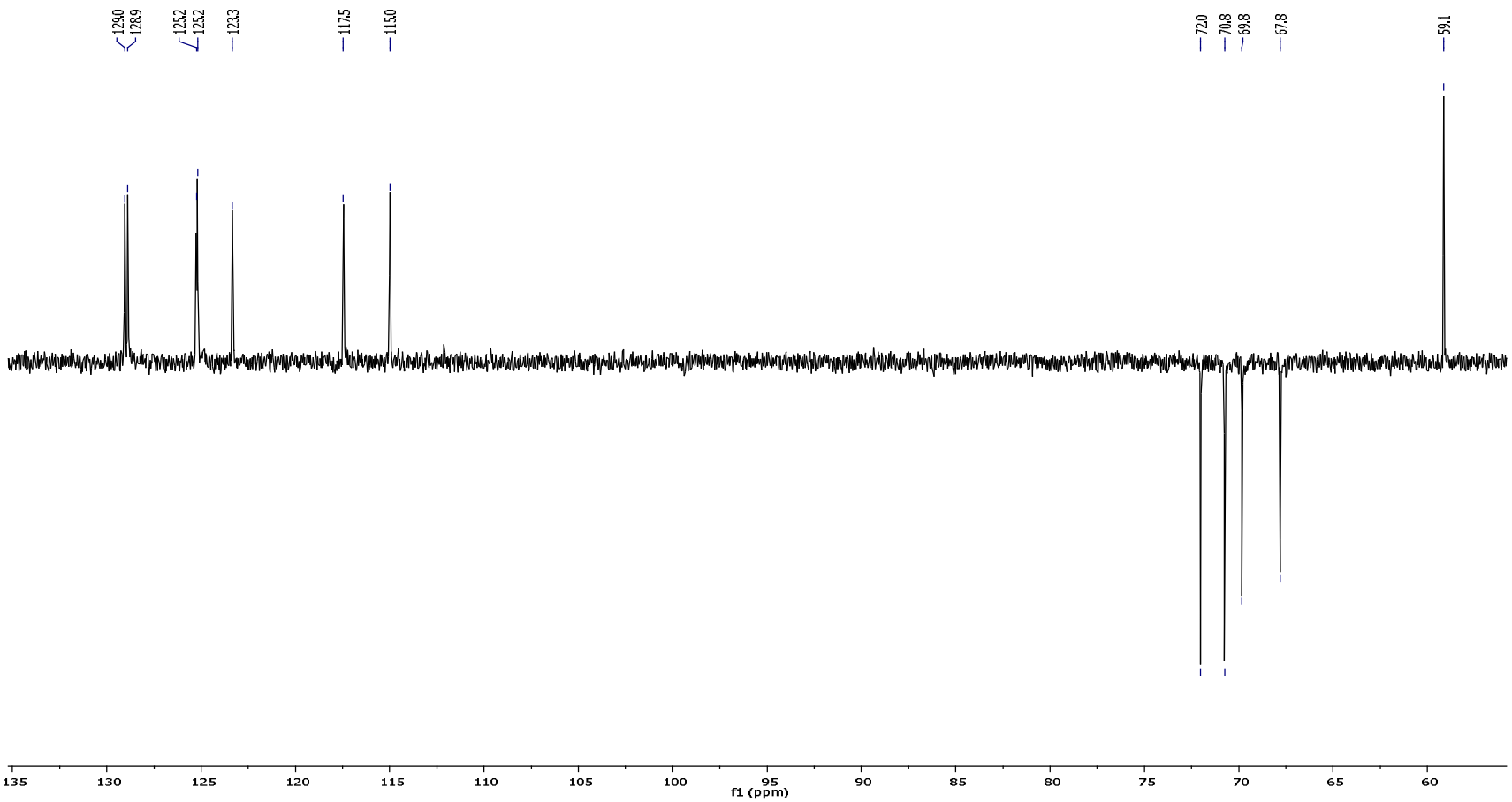

Appendix.19. DEPT-135 spectrum of 5,8-bis(5-bromothiophen-2-yl)-2,3-bis(3-(2-(2-methoxyethoxy)ethoxy)phenyl)-quinoxaline (**50**).